Microstructures and Mechanical properties of AA-5754 and AA-6061 Aluminum alloys formed by Single Point Incremental Forming Process

Sahand Pourhassan Shamchi

Submitted to the
Institute of Graduate Studies and Research
in partial fulfillment of the requirements for the Degree of

Master of Science
in
Mechanical Engineering

Eastern Mediterranean University
September 2014
Gazimağusa, North Cyprus

Approval of the Institute of Graduate Studies and Research

Prof. Dr. Elvan Yilmaz
Director

I certify that this thesis satisfies the requirements as a thesis for the degree of Master of Science in Mechanical Engineering.

Prof. Dr. Uğur Atikol
Chair, department of Mechanical Engineering

We certify that we have read this thesis and that in our opinion it is fully adequate in scope and quality as a thesis for the degree of Master of Science in Mechanical Engineering.

Asst. Prof. Dr. Ghulam Hussain
Supervisor

Examining Committee

1. Prof. Dr. Fuat Egelioğlu
2. Prof. Dr. Majid Hashemipour
3. Asst. Prof. Dr.Ghulam Hussain

ABSTRACT

Single point incremental forming (SPIF) process is considered as a cost-effective method to fabricate sheet metals because there is no need for dedicated dies which are used in other conventional processes. Due to the capability of forming sheets on CNC machines, the flexibility of this process is high which allows the operator to modify the geometry of the product much easier than the other methods like stamping. This study is carried out to investigate the effects of different forming parameters on the mechanical properties and microstructures of formed parts. The effects of wall angle, feed rate, spindle speed and lubrication are explored on AA5754 and AA6061 Aluminium Alloys. Tensile tests and optical microscopy are used to observe the effects of each forming parameter on the properties of the final parts.

The results show that the wall angle has a major effect on the strength of the formed part. By increasing the wall angle, the strength, average grain size and the chaining of second phase particles increase; however, the amount of elongation decreases in both materials. Also, by increasing the feed rate, the strength and average grain size increase, but it has almost no effect on the elongation of both materials. The spindle speed has the least effect on strength and average grain size of both materials, but a slight increment is observed on the elongation in AA5754. To examine the effect of lubricant, hydraulic oil and grease are used on the AA5754 Aluminium Alloy. The results demonstrate that the strength of the part increases with the use of grease instead of hydraulic oil. Additionally, the average grain size in the part formed by grease is greater than of that formed with hydraulic oil.

From the results, the wall angle and the feed rate are the most significant parameters affecting both microstructure and mechanical properties in SPIF process.

Keywords: Single Point Incremental Forming, Mechanical properties, Microstructures, Wall angle, Feed rate, Spindle speed, Lubricant, Tensile test, AA5754, AA6061

ÖZ

Tek noktalı artan şekillendirme işlemi, sacları üretmek için ucuz bir yöntem olarak kabul edilir, çünkü diğer geleneksel yöntemlerde kullanılan özel kalıplara gerek yoktur. CNC makinesi yardımıyla çalışan bu işlem, esnekliği yükseltmiştir, ürünün geometrisini pres gibi diğer yöntemlerden daha kolay değiştirebilir.

Bu çalışma şekilli parçaların mekanik özelliklerini ve mikroyapılarını farklı yapan parametrelerin etkilerini araştırmak için yapılmıştır. Duvar açısı, ilerleme hızı, iş mili hızı ve yağlama etkisi, AA5754 ve AA6061 üzerinde incelenmiştir. Gerilme testleri, ve optik mikroskopi nihai parçaların özelliklerine etkisini görmek için kullanılmıştır.

Sonuçlar duvar açısının, şekillendirilen parçanın gücü üzerinde büyük bir etkiye sahip olduğunu göstermektedir. Duvar açısını artırmak, ortalama tane büyüklüğü ve materyalin gücünü artırır, ancak uzama miktarı her iki malzemde azalır. Bununla birlikte, besleme hızı, parçanın gücü ve ortalama tane boyutu artmıştır, ancak malzemelerin uzaması üzerinde çok az etkisi görülmüştür. İş mili hızı, güç ve her iki malzemenin ortalama tane boyutu en az etkiye sahip olduğu görülmüştür. Ayrıca, hafif bir artış AA5754 uzama miktarında görülmüştür. Yağlayıcı etkisini incelemek için, hidrolik yağ ve gres, şekillendirme sırasında kullanılmıştır. Sonuçlar göstermektedir ki, hidrolik yağı kullanımı ile parça sağlamlığı artmaktadır, ancak, gres yağı ile oluşturulan parçalarda ortalama tane büyüklüğünün arttığı görülmektedir.

Sonuçlardan yola çıkıldığında, duvar açısı ve besleme oranı, SPIF işleminde mikroyapı ve mekanik özelliklerde en önemli parametrelerdir.

Anahtar Kelimeler: Tek Noktalı Artan Şekillendirme, Mekanik özellikler, mikroyapılar, duvar açısı, besleme oranı, Mil hızı, yağlayıcı madde, çekme Testi**,** AA5754, AA6061

DEDICTATION

To my beloved Grandfather:
Who recently passed away.

ACKNOWLEDGMENT

First, I would like to state my sincere gratitude towards my supervisor Assist. Prof. Dr. Ghulam Hussain for his kind support and vital guidance during this work.

Also I very much appreciate the efforts made by Prof. Dr. Majid Hashemipour and Prof. Dr. Fuat Egelioğlu in reading and correcting this thesis. Moreover, thanks to the all academic members and lecturers during my master program who helped me to expand my knowledge and perception in this field. I also appreciate the helps of Khosro Bijanrostami for his assistance in practical part of this study and many thanks to my friend Besong Lemopi.

And of course my precious family for their enormous supports and endless love and I will never forget their sympathy and affection.

TABLE OF CONTENTS

LIST OF TABLES

LIST OF FIGURES

LIST OF SYMBOLS AND ABBREVIATIONS

Abbreviations /symbols	Meaning
AA	Aluminium Alloy
SPIF	Single Point Incremental Forming
TPIF	Two Point Incremental Forming
CAD	Computer Aided Design
CAM	Computer Aided Manufacturing
OM	Optical Microscope
FLC	Forming Limits Curve
CNC	Computer Numerical Control
Mg	Magnesium
Si	Silicon
Al	Aluminum
Cu	Copper
Fe	Iron
HF	Hydrofluoric Acid
HNO_3	Nitric Acid
HCL	Hydrochloric Acid
$\bar{d}$	Average grain diameter
$\bar{A}$	Average grain area
l	Mean linear intercept length
ASTM	American Society for Testing and Materials

Chapter 1

INTRODUCTION

1.1 Background for Aluminium Alloys

Among the materials which have been used in sheet metal forming Aluminium, steel, stainless steel and magnesium alloys are consistently being used in the industry. Aluminium possesses one third the density of steel (2700 kg/m3), however with such low density it possesses high strength and would decrease the weight of the structure when compared with steel. Aluminium alloys with variety of properties are mostly utilized in aircraft and automotive industries. Currently there are 8 series of Aluminium alloys with different principal elements [1,2].

1xxx series: Also known as Commercially Pure Aluminium, the chief characteristics of these series are: work hardened ability, corrosion resistance, and conductivity to electricity, better formability and weld ability. The ultimate tensile strength of these series are between 70-185MPa. Regularly 1xxx series have been used in applications where formability and resistance for corrosion are required, such as electrical conductors [3].

2xxx series: The main element is Copper. The ultimate tensile strength of these series are around 190-430MPa. For some alloys in these series it is required to use mechanical joints rather than welding but others may be exempted from this restriction. These series of alloys could be used in aircraft and truck body.

3xxx series: The main alloy element in these series is Manganese, and it helps the alloys to be more ductile. These alloys have high corrosion resistance and high formability. The ultimate tensile strength of these series are around 110-285MPa. Weld ability of 3xxx series make them suitable for home appliances and chemical equipment.

4xxx series: Due to the Silicon as a main element, these series are low ductile alloys. These Aluminium series may have increased strength with heat treatment and their ultimate tensile strength are around 175-380MPa. These alloys have been used in automotive industry as a medium to weld the auto body structures, because of its fluidity for welding. Usually 4xxx series are used in foundries for casting where high fluidity and low ductility is required.

5xxx series: Generally, Magnesium as a chief element increases the weld ability plus nearly no loss in strength. These series are famous for their exceptional corrosion resistance, weld ability and toughness. Mostly used as buildings, automotive and marine industries. The ultimate tensile strength of these series is 125-350MPa. Additionally 5754 can be used as an exterior panel for automobiles because of their great formability [4,5].

6xxx series: Alloys in which Magnesium and Silicon are main elements, plus these alloys are machine-able, heat treatable and have great corrosion resistance and high extrude-ability. Their ultimate tensile strength are about 125-400MPa.Formability and weld ability for these series are high. Because of their fine attributes, they are used in automotive, exterior panels and marine industries as well as construction applications.

7xxx series: Zinc is the principal element for heat treatable alloys, and has the highest strength among the other alloys. Heat treatability and high toughness are other features of 7xxx series, thus the ultimate tensile strength is about 220-610MPa. Because of their remarkable strength, 7xxx series are extensively used in aerospace industries [6].

8xxx series: Mostly includes lithium composition, which has heat treatability, great conductivity and strength and hardness. Based on the lower density of Lithium when compared to Aluminum, it have better solubility and it may alloy with Aluminium to improve the stiffness and age-hardening of the material. The ultimate tensile strength of these series is around 120-240MPa. Al-Li alloys are used for aerospace applications.

1.2 Motivation

Nowadays, there has been a growing requirement in the industry that needs agile and flexible manufacturing methods. Due to the various customer demands, it is a great challenge to support production of the desired products, and still make profits. In conventional sheet metal forming techniques, which are used mostly in mass production, high initial cost for equipment is needed. Single point incremental forming (SPIF) has shown capability to respond changing market demands and is appropriate for batch productions and rapid prototyping. The process is not similar to other sheet metal forming methods (e.g. stamping or deep drawing) here there is no need for a die. Therefore, there would be a considerable saving because of reduction in tool cost and lead time as well as non-existence of special die. So, SPIF is economic and cheap for a batch of production. The whole process can be guided by CNC machine or by robot, though the forming time is longer with respect to

conventional sheet metal processes. But it would be an excellent option for fabricating the prototypes and intricate parts in aeronautical, automotive and medical purposes [1].

1.3 Scope and Objective

The objective of this thesis is to execute experimental investigations on SPIF process to observe the strength, ductility and microstructures of Aluminum alloys. Two kinds of Aluminium alloys were used namely AA5754 and AA6061 with the same sheet thickness of 1.5 mm. The current study involves a series of experimental explorations related to the effect of different parameters on Aluminium alloys to spot the changes in mechanical properties as well as microstructure along the rolling direction with the assistance of optical microscopy and tensile testing machine. In this study, effects of wall angle, feed rate, rotational speed of spindle and lubrication were investigated at room temperature and other parameters (e.g. tool radius, step size, tool path, lubrication and sheet thickness) remained constant during the experimental practices.

1.4 Organization of the Thesis

This thesis is divided into 5 chapters including the introduction and conclusion which summarize the main contribution and results of the current study.

Chapter 2 commences with the classification of manufacturing processes and ends up with the sheet metal forming as a member of metal forming process. Most well-known sheet metal forming processes are discussed along with the general information about incremental forming process. In particular, single point incremental forming process has been discussed including formability, forming

defects, effective process parameters as well as theoretical background of the SPIF process and current applications.

Chapter 3 covers the experimental plans and CAD/CAM design of the parts in this study. The material properties, machine tool, forming geometry, clamping system and data collection method have been discussed in this part.

Chapter 4 presents the results of the tensile tests and optical microscopy of the formed parts. It discusses the effects of wall angle, feed rate, spindle speed and lubrication on mechanical properties and microstructures.

Chapter 5 includes the conclusion of this work.

Chapter 2

LITERATURE REVIEW

2.1 Classification of Manufacturing Processes

It has been proven that geometry, tolerance, production rate and environmental aspects are all considered as the main attributes of manufacturing processes. Generally, to deal with metal forming from an initial blank or casted material, there are five distinct methods of manufacturing processes that would be helpful to produce the final product with desired shape, accuracy and tolerance [1]. The five manufacturing methods are: Primary shaping processes, Material removal process, material treatment method, joining process and forming processes.

2.2 Sheet Metal Forming Processes

2.2.1 Spinning Process

It is known that spinning is an ancestor of incremental forming, sometimes called spin forming, and is a fairly simple process for manufacturing the axisymmetric parts. The whole process starts by clamping the blank among tailstock and mandrel, and the blank is supposed to be rotated at high speed with the mandrel. The mandrel forms the shape of the inner side of the hollow-like final product. Meanwhile, the roller tool presses the sheet toward the mandrel by a predefined path while the sheet is rotated by spindle. The roller wheel takes few passes to fabricate the product. In conventional spinning process, the sheet undergoes an incremental force over the mandrel by a tool. Shear spinning has distinct difference with conventional one, in

this method the blank is stretched rather than bent, by applying a downward force to the sheet [7].

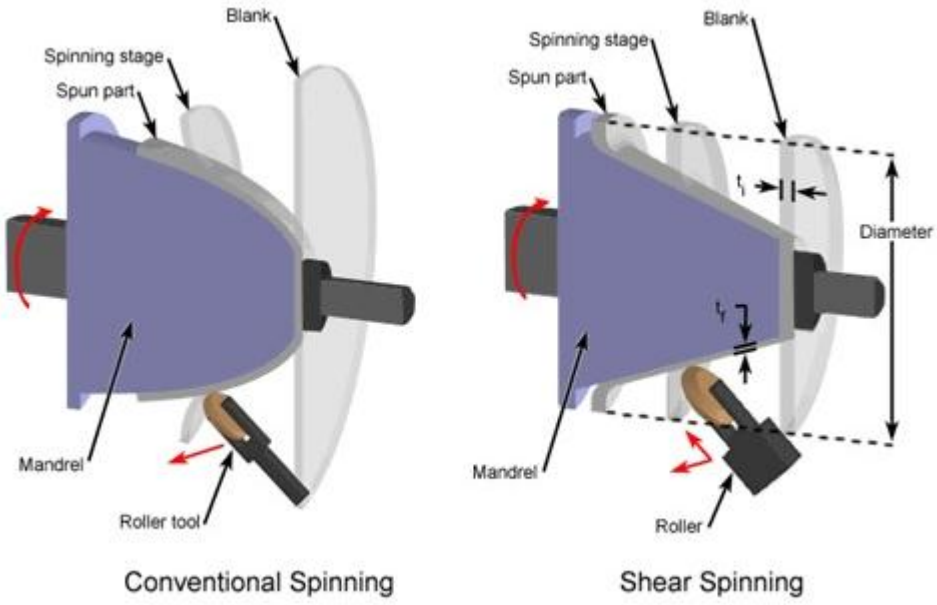

Figure 2.1: Conventional and shear spinning [7]

Advantages of this process include high precision, very low wearing in mandrel and tool, and the process can be done either manually or by CNC.

2.2.2 Stamping

The process of stamping is an appropriate solution for fabricating products with high volume and minimum diversity (mass production). This sheet metal forming process is based on dies which made a final shape of the sheets.

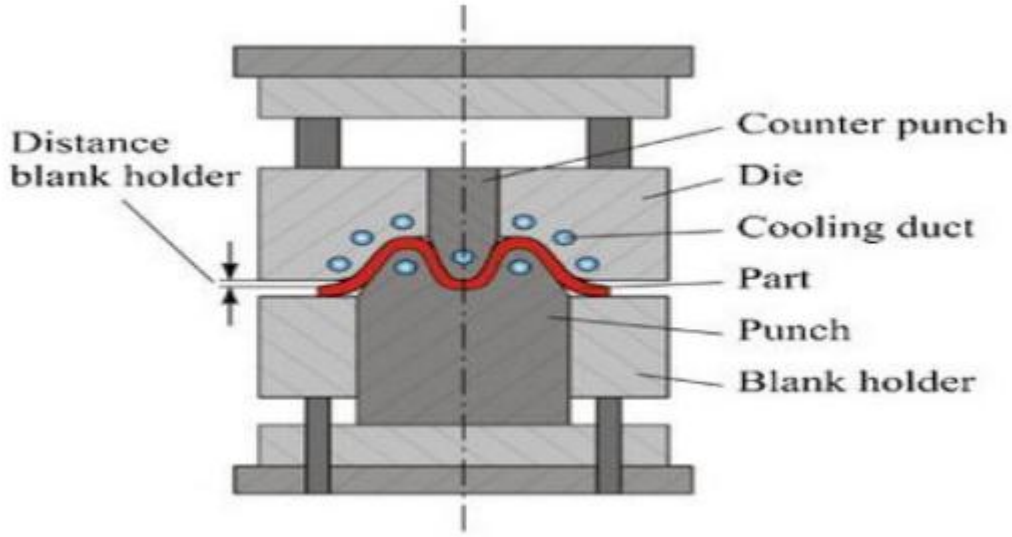

Figure 2.2: Tool design for Hot Stamping Process[8]

Formability in this process relies on the ability to bend, drawn as well as stretch. The die refers to the tool that is used in stamping and it includes male and female parts which are responsible for the forming. The apparatus of stamping are mechanical and hydraulic presses. As the drawbacks for stamping process, the tools are costly and needs regular maintenance. Besides, the price of die is expensive which will elevate the total cost of the machine [8].

2.2.3 Incremental Sheet Forming

In factories which deal with mass production, deep drawing is considered as an alternative process for sheet metal forming. However, due to the various demands, high initial cost and lead time for making appropriate dies, sheet incremental forming emerges as an ideal solution in order to fabricate small batches of production and rapid prototyping [9].

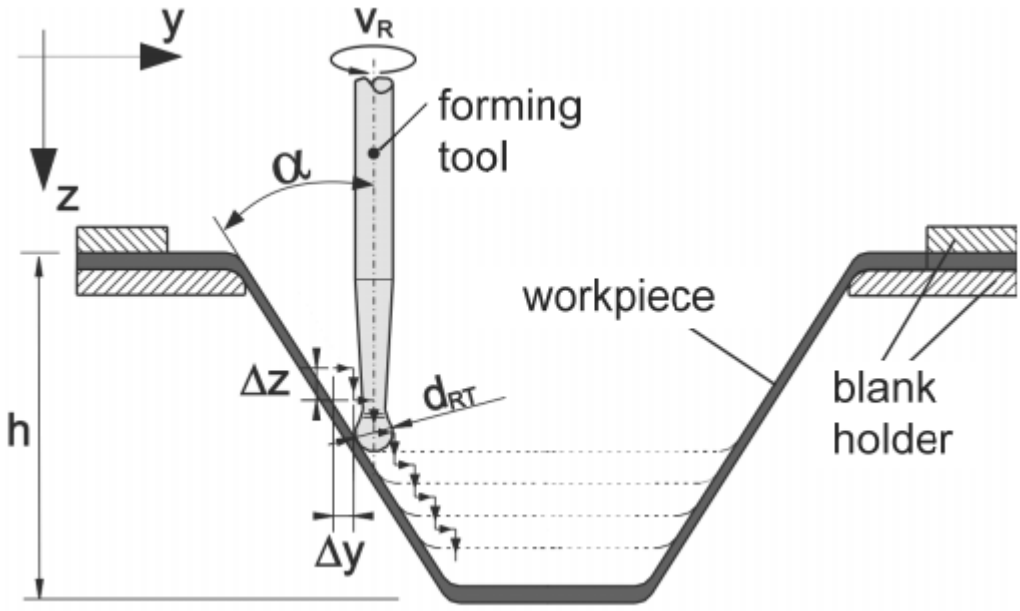

Figure 2.3: Schematic representation of SPIF [9]

Incremental Sheet Forming is known as a process in which plastic forming occurs locally, the tool which is supposed to form a blank by predefined path gradually cover the entire part. Sheet incremental forming has the possibility to be carried out by computer numerical controlled (CNC) machine which follows a tool path [10].

Sheet incremental forming has considerable advantages like die less nature of the process which decrease the initial cost, also the process can be implemented by any universal milling machine with minimum 3 axis control system. Moreover simple hemispherical tools can be used as a forming tool during the plastic forming.

2.3 Classification of Sheet Incremental Forming

The categorization of incremental forming process is based on method of forming and it consists of Single Point Incremental Forming (SPIF), Two Point Incremental Forming (TPIF) processes and Incremental Forming with Counter Tool [11].

2.3.1 Single Point Incremental Forming

This method, which is often referred as a negative incremental forming, is frequently utilized to form the sheets by CNC machines. The first contact between the tool tip

and blank starts at the border of the lower plate (outer area) and gradually goes down to the center by following the tool path. The blank is fixed by a blank holder (fixture) and in each time only a small portion of the blank is formed by the forming tool of the CNC milling machine, however, in some other cases a dedicated rig or back plate may be utilized during the forming process. The figure 2.4 below illustrates the both with and without the rig [11].

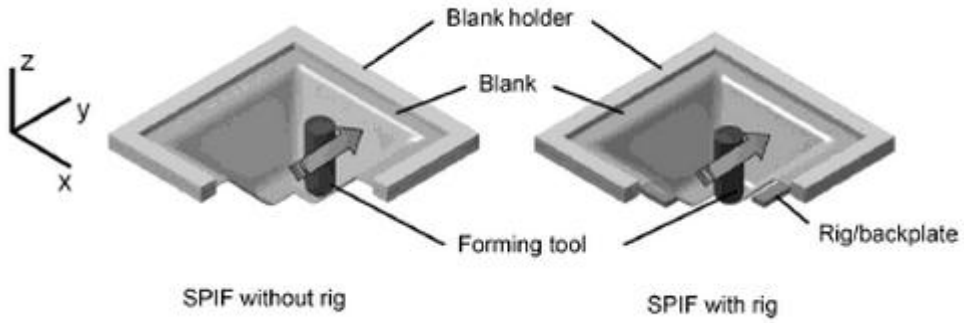

Figure 2.4: Classification of single point incremental forming [2]

2.3.2 Two Point Incremental Forming

In this process, full die or partial die is employed as in positive incremental forming. The main idea behind the usage of secondary dies in TPIF is to achieve higher precision of manufactured parts and also to handle complex geometries. This approach is same like the SPIF, the blank must be fixed by a fixture and a forming tool can be employed to start the forming process. On the other hand, the tool tip commences the forming from the center of the sheet by following counters of the tool path.

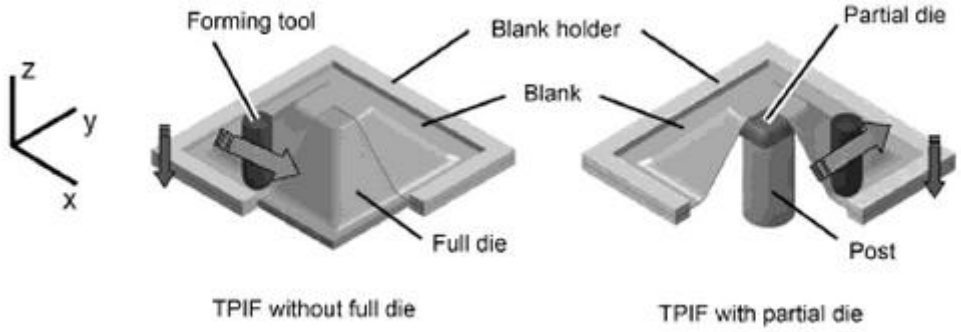

Figure 2.5: Classification of two point incremental forming [2]

2.3.3 Incremental Forming with Counter Tool

This is another method of incrementally fabricating sheets and it is completely die less with the help of counter tool, which follows the same trajectory of the main one. Thus this process is more flexible with comparison of other Incremental Sheet forming (ISF) methods.

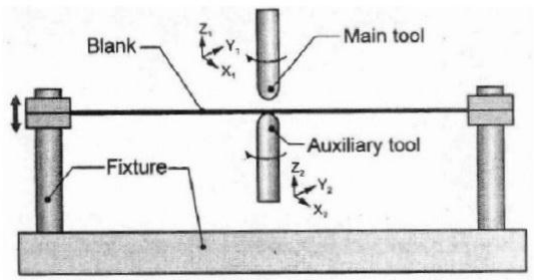

Figure 2.6: Incremental sheet forming with counter tool [2]

2.4 Theory of Forming Limits on SPIF

The term of formability has been regarded as a crucial and complex issue for SPIF. At first, it was presumed that the only criterion to predict the formability was the wall angle of the final product, but it is not sufficient to obtain the intricate strain states during the ISF process. Thus, according to the sine law thickness of the part can be estimated before the process [12].

The thickness of the sheet will reduce by the increasing the wall angle of the part. So, depending on the material properties of each sheet, there will be a limit for wall angle for each sheet based on their material properties [13, 14]. Therefore, the limit of formability can be identified by this method. Clearly, foretelling the boundaries of formability in SPIF is very complicated. Thus, Forming Limits Diagram (FLC) which initially has been utilized for conventional methods in sheet metal forming deemed as a proper way to exploring the optimum wall angle. In this regard, forming limits for traditional sheet metal forming methods was investigated by Nakajima [15] and Marciniak [16] approved by metal forming society.

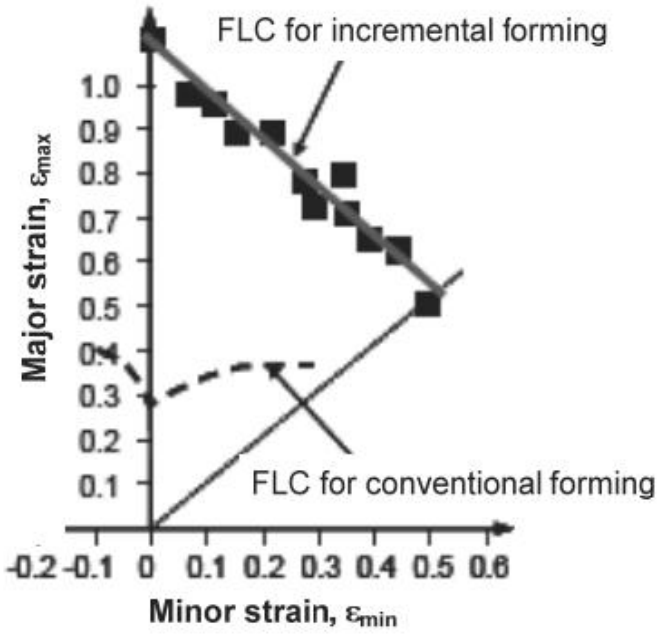

Figure 2.7: FLC comparison between the conventionally and the incremental sheet forming [9].

As can be seen in figure 2.7, it is very clear that the formability of the single point incremental forming process is higher than the other conventional forming methods because of the highly localized plastic deformation zone during the process which also causes an extension on the part geometry.

2.5 Forming Defects

One crucial criteria of incremental forming is to withstand the plastic deformation during the forming process. Much research has been done over the formability of ISF and fracture predictions. Generally, there are 3 different types of failures for this process, which are listed below [17]:

Squeezed-out wall formation

This defect appears due to unequal ratio of tool diameter and sheet thickness, so for small tool size, the interaction with the blank causes severe contact force and squeezing out the sheet. Occurrence of this defect is independent from the geometry of the part, figure 2.8 (A).

Corner fold

Corner fold occurs only in parts with corners, figure 2.8 (B), and this defect happens for parts formed with lower diameter tools with respect to the blank thickness. So the result would be a fold in the material.

Bulge height

It is also called pillow effect in the final product, and especially exhibited at the base of parts made with lower wall angles.

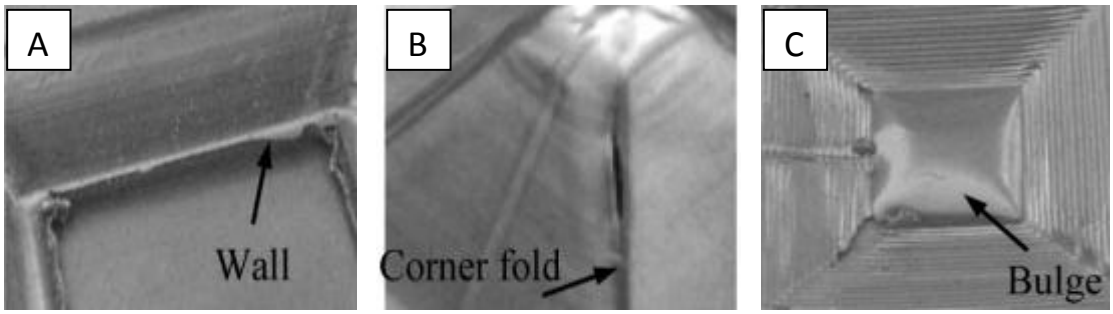

Figure 2.8: Forming defects for Incremental Sheet Forming [17]

Therefore, due to the plane stresses, pillow effect occurs during the process and it is not dependent on the geometry of the part, figure 2.8 (C). Basically, defects mostly take place because of close interaction between tool diameter and blank thickness and consequently failure would decrease the formability of the product. Among these defects wall and corner fold defects depend on the increase of step size, wall angle and initial blank thickness [18].

2.6 Process Parameters

It is believed that in SPIF process there are diverse factors which have impact on the outcome of the process. Parameters like wall angle, tool diameter, feed rate and step size could have the considerable effect on the strength, formability and surface finish of the parts.

According to Ham and Jeswiet [19] vertical increments (Δz), speed of spindle, feed rate and wall angle affect formability of SPIF and by increasing the rotation speed of spindle, formability will get better. Tool diameter and depth of part have no effect on forming; However, Bhattacharya et al. [20] mentioned that by increasing the tool diameter formability will reduce, and for the surface quality, increasing in tool diameter and higher inclination on wall angle causes to reduce the surface roughness.

2.6.1 Forming Tool

The tools that are used in the process are solid; however some other researchers investigated the water jet as a forming tool. Normally tools are made from high speed steel (HSS) and based on demand rather than buying from the market. For SPIF method, it is usual to use solid hemispherical head with shorter shank in sharp wall inclinations to eliminate the collusion between tool and blank. The ball tool is more effective than the hemispherical head tool in terms of formability. Kim and Park [21]

indicated that those tools which have hemispherical tips possess better formability that ball headed tools. The diameter of tool is another important issue over the formability, and it affects the deformation. With the higher diameters of tool, there is a possibility to expand the strain through a larger area, therefore lower strain is expected. So as a conclusion, with higher tool diameters, surface roughness will decrease and on the other hand, maximum wall angle which characterize as a formability limit will reduce [22].

2.6.2 Tool Path Generation

Tool path generation has critical influence on the SPIF, such as: accuracy, surface roughness, process time and of course formability.

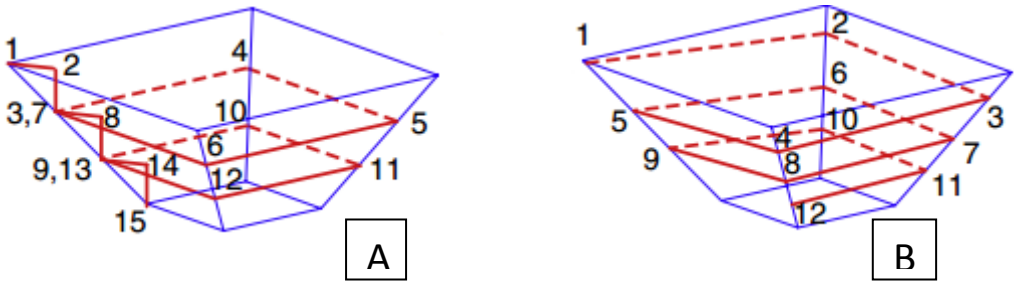

Figure 2.9: Constrain and helix method for tool path generation [23]

One method is counter tool path, which is also known as constant Δz, figure 2.9 (A), in this method for each vertical feed, there is a horizontal movement along the periphery of the part. On the other hand, in helical tool paths, figure 2.9 (B), the tool travels along the periphery with helix shape and vertical depth of each loop is equal to incremental depth. Between the two methods for tool trajectory helical tool path shows homogeneous thickness distribution and no scarring on the transition points.

2.6.3 Feed Rate

It is clear that the forming process has higher feed rate in comparison with machining processes. But higher feed rate, which leads to high friction and temperature between

the forming tool and sheet metal, can destroy the surface quality of the product. According to Kim and Park [21] and Strano [24] in order to improve the formability, feed rate should be decreased. Thus it is better to take a lower feed rate in the process.

2.6.4 Lubrication

It is believed that proper lubrication will reduce the amount of friction of forming tool as well as account for better surface quality of parts. The existence of partial friction between the tool and the sheet metal assists process formability [25]; however, Strano et al. [26] revealed that formability will reduce by high friction during the SPIF process.

2.6.5 Step Size

It is also called the vertical feed rate (Δz) and it is controlled by z axis of CNC machine during the forming process. As can be seen in figure 2.10, the amount of vertical increment on each path is defined as a step size in SPIF process.

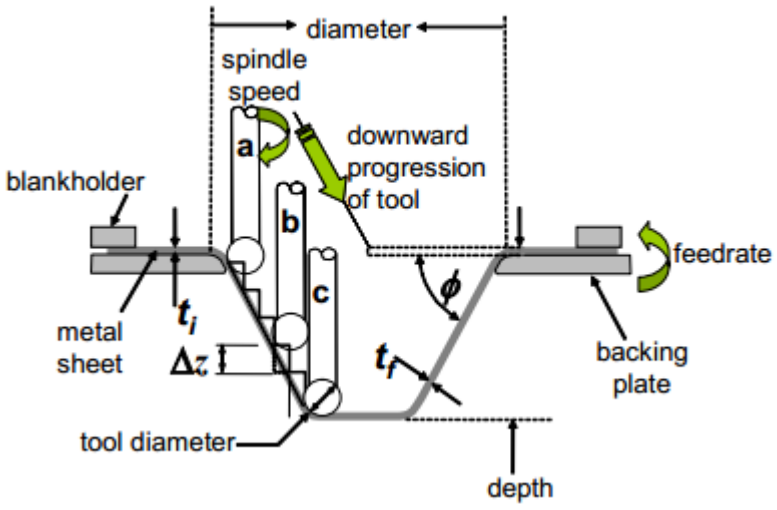

Figure 2.10: The step size and the wall angle parameters in the SPIF process

This parameter has an effect on the final surface of the product. Step size has critical consequence on part accuracy as well as being smooth in surface of the desired final shape. Step size has no effect on formability, but it involves the surface finish of both inner and outer side of the part, however, to get good surfaces there should be less vertical increments and that means more time is needed to form the part [27].

2.6.6 Spindle Rotation

Because of the friction between the blank and the forming tool, speed of spindle rotation (RPM) is considered as a formability parameter. So, in order to improve the formability of sheets in the SPIF process, high rotational speed of spindle is proposed. However, some other drawbacks may appear regarding high RPM during the forming process. For instance, lower surface quality and reduction in tool life due to excessive wear rate. So higher spindle speed might affect the fabricated part to become wavy on its surface [28,29].

2.6.7 Wall Angle

The figure 2.10 shows the location of wall angle (ϕ) on SPIF. The term of formability depends on the maximum wall angle in which a sheet can carry without failure. The limit of wall angle has a close relation with material properties and initial thickness of the blank. Wall angle could be measured by a tangent line between the blank and formed surface. Among the ways to predict the formability of a sheet metal, the Cosine's law and FLC diagram could be utilized and it is experimentally proven that the formability of the sheets which are made by SPIF is much higher than those formed by conventional methods (e.g. stamping and deep drawing). It is known that by increasing the wall angle (steeper inclination), the thickness of the formed part decreases [30].

2.7 Applications of Incremental Forming Process

Generally SPIF process has been used in rapid prototyping and batch productions. The main idea of IFP is to deal with prototypes during the design stage to reduce the cost of expensive forming dies and to get the quick evaluation over the samples [31]. For instance, in automotive industries parts like exterior panels, reflexive surface to lights and heat and vibration shields could be produced with acceptable accuracy without dedicated die. As can be seen in figure 2.11 the hood panel was made by Amino et al [32] as a replacement component for the hood panel of Honda sport car.

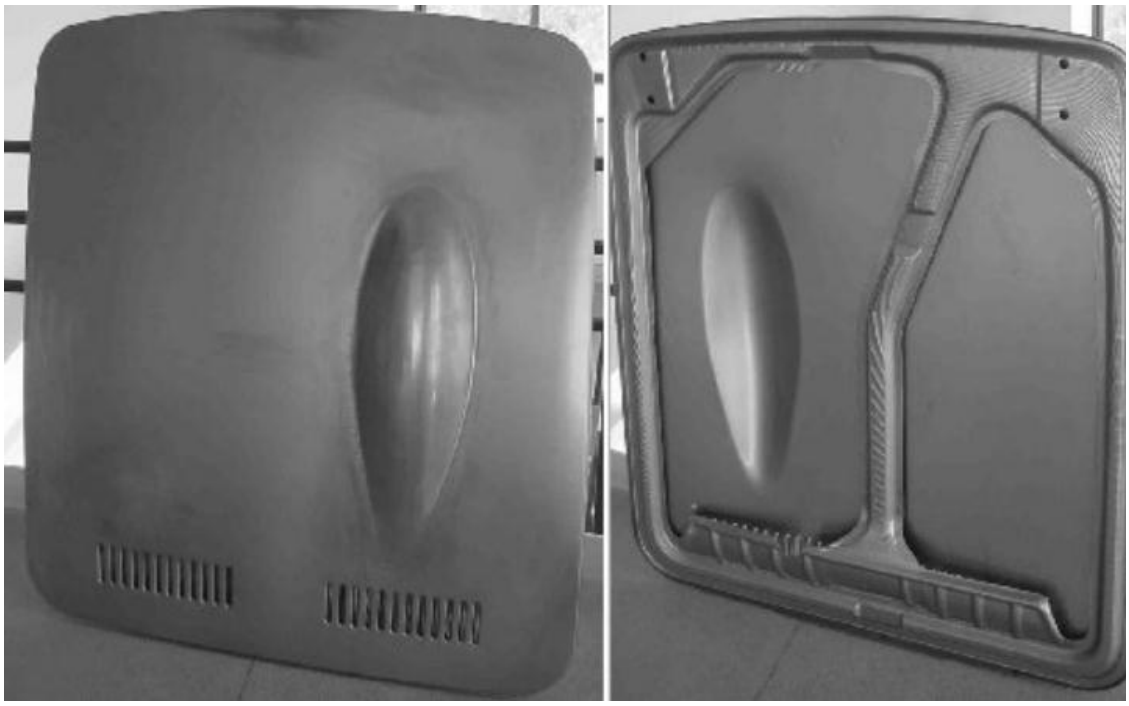

Figure 2.11: Honda hood panel fabricated by IFP[32]

Figure 2.12: Automotive heat/vibration shield [33]

Chapter 3

METHODOLOGY

This section provides the experimental procedure that is used in this research. The experimental conditions and motivations behind selecting the materials, Aluminium 6061 and 5754, are given. Also the methods for identifying the material properties and microstructures of formed parts were included with the outline of the experiments and CAD/CAM design for running the experiments.

3.1 Plan of Experiments

The variables are changed during the experiments in order to find their effects on two different types of Aluminium alloys used in this study. As can be seen in table 3.1 the effect of the forming angle was investigated by varying from the steeper one to shallow one, (i.e.55°, $45^{\circ}$and 35°). In addition, the feed rate is altered from 1000mm/min to 4000mm/min for both of the materials using the same direction of the tool path. Also the rotational speed of spindle was altered in order to observe its effect on the surface quality of final product and also on microstructure. The spindle speed ranged from 50 RPM to 1000 RPM.

Other parameters where held constant during the experiment. One of them, which has a high influence in part accuracy and better surface quality, is vertical feed rate (step size). It was defined when generating the tool path. Thus, the constant value for step size was 0.5mm. The blanks used in the SPIF process were 1.5 mm in thickness for both AA5754 and AA6061. For lubrication, all of the experiments were done

using proper lubricants to avoid any wear between forming tool and blank and also to obtain the smooth surface quality. The forming tool during the process was 14mm in diameter. Last a helical tool path was used for all of the experiments.

Table 3.1: Test plan of for AA6061 and AA5754

Material	Forming Angle	Feed rate (mm/min)	Rotational speed (RPM)
AA6061 AA5754	55°	2000	1000
	35°	2000	525
	35°	1000	525
	35°	4000	525
	35°	2000	50
	35°	2000	1000
	45°	2000	1000

Table 3.2: Test plan to investigate the effect of different lubricants

Material	Forming Angle	Feed rate (mm/min)	Rotational speed (RPM)	Lubricant
AA 5754	35°	2000	1000	Hydraulic oil
	35°	2000	1000	Grease

3.2 CAD/CAM Design

The current study was carried out in order to obtain the mechanical properties and characteristics of the blank after plastic deformation and variation in the grain sizes along the rolling direction of each Aluminium sheet which was used. In this regard, a proper method for defining the tool path in CAM software is necessary. All of the parts were formed in a pyramid shape with 180mm×180mm dimension (working area).

In SPIF there are two common methods used for specifying the tool path for the process, (i.e. constrain and helical method). Constraint method provides a constant vertical feed rate on each contour along the periphery of working area, however, with the helical tool path there is a constant change in variables for each axis (X, Y and Z), this leads to improve surface quality, particularly scratch along the corner of the part [34]. Three different wall angles were selected to investigate the formability of the materials. Also, a step size of 0.5mm was chosen for the vertical feed rate. After creating the G codes, CIMCO software was used to simulate the whole forming process to make sure that codes were correct. The step size is not considered as a formability parameter, however, it determines the surface quality, and a smooth surface finish can be obtained by decreasing the vertical incremental [35].

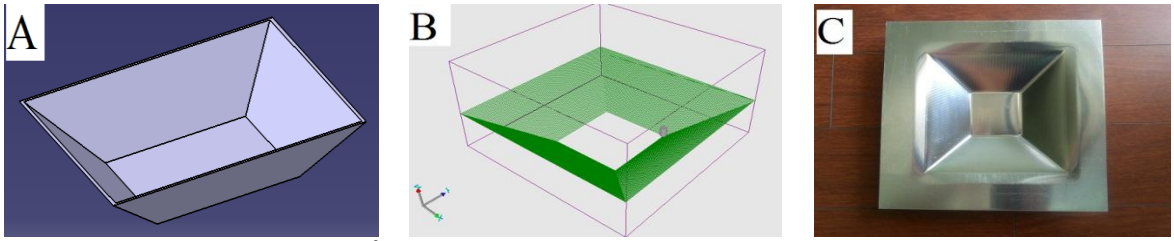

Figure 3.1: Pyramid with 35° wall angle, (A) CAD design of the part, (B) CAM tool path simulation, (C) Actual formed part

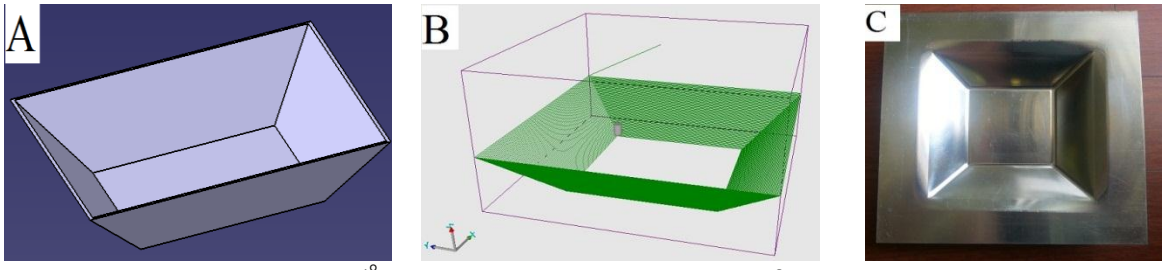

Figure 3.2: Pyramid with 45° wall angle, (A) CAD design of the part, (B) CAM tool path simulation, (C) Actual formed part

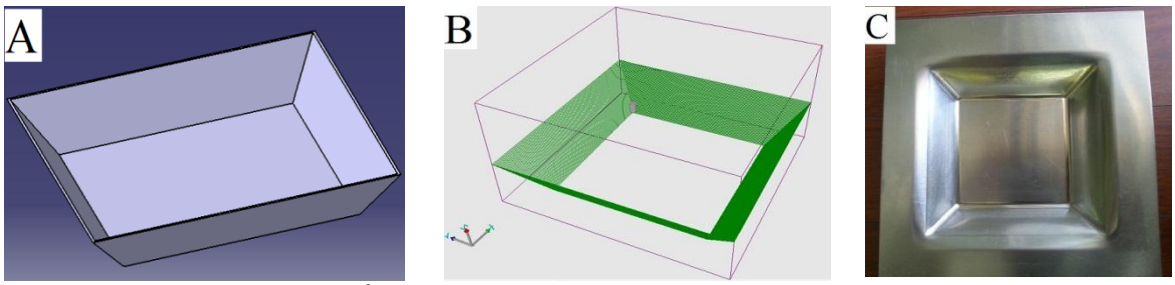

Figure 3.3: Pyramid with 55° wall angle, (A) CAD design of the part, (B) CAM tool path simulation, (C) Actual formed part

3.3 Experimental Setup

In this part the experiments will be explained which consists of CNC milling machine, forming tool used in process, clamping and lubrication.

3.3.1 The CNC Machine

The whole forming processes have been carried out in the CAD/CAM laboratory of the Mechanical Engineering in Eastern Mediterranean University. As can be seen in

figure 3.4, the CNC milling machine with 3 axis which made by Dugard was utilized to fabricate the pyramids on this study.

Figure 3.4: Dugard ECO 760 CNC milling Machine

Table 3.3: Technical specifications of CNC machine

Operating system of CNC	Fanuc OiMD
Number of axis of freedom	3
Machine capacity (maximum travel on X,Y,Z) mm	760, 430, 460
Spindle speed	8000rpm (opt 10,000rpm)
Rapid feed rate on X,Y,Z mm	24 / 24 / 24 m/min
Cutting feed rate	10m/min
Max tool diameter with adjacent tool	100

3.3.2 Forming Tool

In order to investigate the other parameters, the tool diameter and the tool tips were held constant during the experiments. The tool is made from high speed steel (HSS) and hardened up to 55 HRC with the diameter of 14mm. The geometry of tool tip is hemispherical to reduce the friction between the blank and forming tool. The figure 3.5 shows the only forming tool in this experiment with its holder on CNC milling machine.

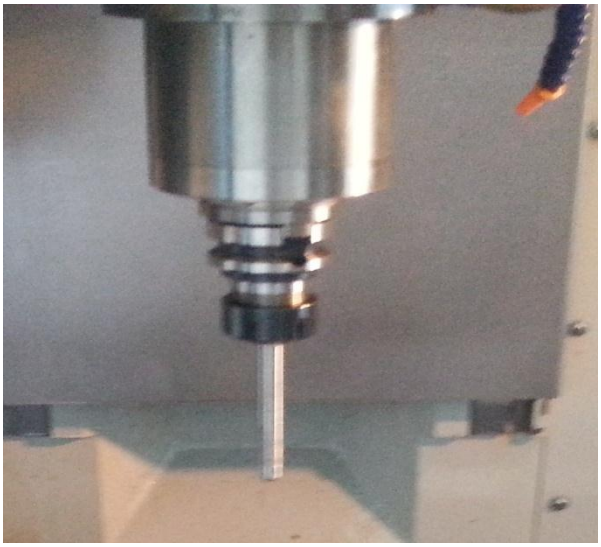

Figure 3.5: The forming tool and the tool holder

The motivation behind choosing the tool with 14mm diameter is because of the formability issues. Tools with higher diameters tend to distribute the strain over the larger area on the blank, therefore the amount of stain will reduce and as a result surface roughness will decrease [36].

3.3.3 Clamping System

The forming processes have been done by utilizing the clamping system to hold the sheets as can be seen in figure 3.6.

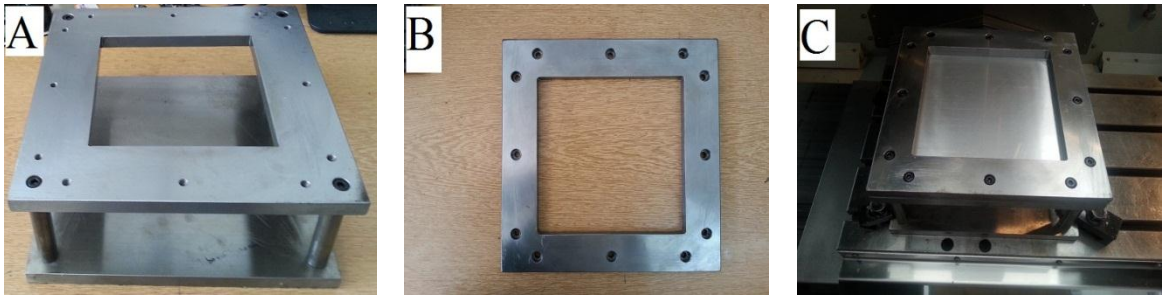

Figure 3.6: (A) Bottom and lower plates, (B) Upper plate, (C) Complete clamping system fixed on machine table

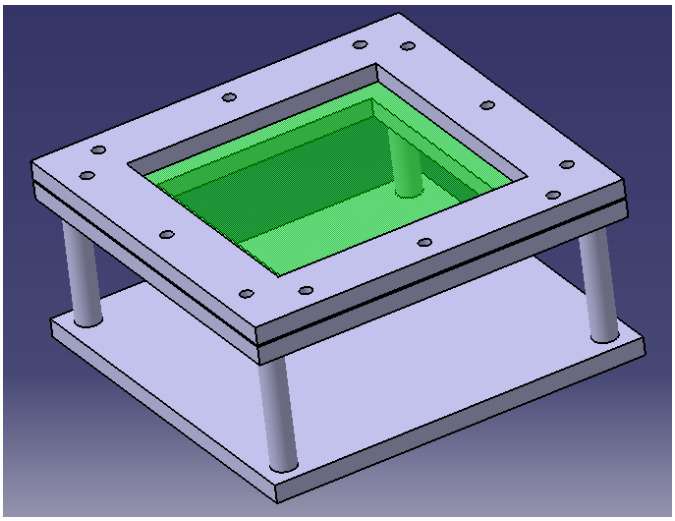
Figure 3.7: The CAD design of complete fixture with fastened sheet on CATIA

The clamping system is shown in figure 3.6 (c). The CAD drawing of assembled fixture is provided in figure 3.7. In order to eliminate early failure during the process, the edge of inner plate was chamfered, since sharp edges have a tendency to increase the stress on sheet. The fixture was made from marine steel and consists of upper and lower plate which are joint mechanically via M8 Counter-bored screws and as can be seen in figure 3.6 the fixture has a bottom, lower and upper plate and four bars which were utilized to lift the lower plate from the table and give enough space for deeper products. Here, the working area is 180mm×180mm (inner dimension of lower plate) and the blank is fastened by using an upper plate above it (with

310mm×310mm inner dimension). During the G code generation for the tool path, coordinates must be defined meticulously with respect to dimension and square frame of the upper plate to prevent any collision which might harm the spindle, the tool and fixture as well.

3.3.4 Lubrication Condition

Lubrication has a great importance in SPIF not only in reducing the tool wear but also for better surface quality that it provides. During the experimental work two kinds of lubrication was used. Almost all of the forming was done by using LG Hydro HD liquid lubrication but in order to investigate the effects of the lubrication Lithium Complex EP2 Grease was also employed in AA5754 material. Table 3.4 provides information related to the physical characteristics of the lithium complex grease.

Table 3.4: Physical characteristics of The Lithium Complex Grease

Appearance	Fibered adhesive grease
Color	Red Sparkle
Dropping point °C	>260 °C
Temperature range in operation °C	-20 to 160
Aluminium corrosion	Negative
NLGI grade (ASTM D 217/DIN)	2

3.3.5 Material Specifications

The experimental work is carried out by two different grades of Aluminium alloys (i.e. AA5754 and AA6061) and both have sheet thickness 1.5mm. The table 3.5 provides information related to the blanks that are used in SPIF process.

Table 3.5: List of materials used in this study

Material	Thickness (mm)	Sheet area (mm^2)	Working area (mm^2)
AA5754	1.5mm	250×250	180×180
AA6061	1.5mm	250×250	180×180

Both sets of the sheets were cut by a guillotine from the initial stock with 1mm×2mm dimension. As can be seen from the table 3.5, 180mm×180mm were used as a working area for the SPIF process, however, the rest of the material were utilized to fastening the blank in dedicated fixture. AA-5754 was chosen for this study because of its high strength as well as low density and it is an important material in the automotive industry. Usually this series of Aluminium alloys is used in structural panels because of their good strength, stretch and acceptable deep drawing characteristics. Hence, AA-5754 is used as a substitute for heavy metals. Besides, it possesses great corrosion resistance and also it is capable of being recycled. The chemical composition of the both materials was tested by the PMI master pro metal analyzer made by Oxford instruments.

Figure 3.8: PMI-Master pro metal analyzer by Argon gas

The chemical composition of AA-5754 Aluminium alloy is provided in the table 3.6.

Table 3.6: The chemical compositions of 5754 Aluminium alloy (Wt. %)

Silicon (Si)	Iron (Fe)	Manganese (Mn)	Magnesium (Mg)	Cupper (Cu)	Titanium (Ti)	Chromium (Cr)	Al
0.087	0.265	0.194	2.42	0.032	0.005	0.046	Bal.

As a second material for this study, AA-6061 is selected because of its availability and its usage in diverse purposes. Generally, this series of Aluminium alloys have been used in outer panel of automobiles due to their great surface quality and formability. Therefore, good mechanical properties, corrosion resistance, high strength and workability which combine with its availability in market made this alloy a proper material for this study. Table 3.7 provides the chemical composition of AA-6061 Aluminium alloy.

Table 3.7: The chemical composition of 6061 Aluminium alloy (Wt. %)

Silicon (Si)	Iron (Fe)	Cupper (Cu)	Manganese (Mn)	Magnesium (Mg)	Chromium (Cr)	Titanium (Ti)	Al
0.60	0.58	0.202	0.042	0.741	0.207	0.052	Bal.

Furthermore, these alloys are perfect in applications with low temperatures due to their toughness, ductility and strength in very low temperatures. After forming the sheets to their final shapes, the microstructures of the formed Aluminium sheets are investigated with an optical microscope to determine the effects of different forming parameters on both AA6061 and AA5754 materials. Figure 3.9 illustrates the optical microscope and polishing device. And other critical issue during the optical microscopy is to find the proper etching solution for both of the material. So according to the ASM Handbook [38], Poulton's reagent (12ml HCL+ 6ml HNO_3+

1ml HF+ 1ml DI water) was used for AA6061 and for AA5754 50ml of abovementioned reagent+ 40ml acid chromic+ 10 H_2O was used as to reveal the grains before and after plastic forming.

Figure 3.9: (A) Optical Microscope (B) Polishing device

Meanwhile, in order to investigate the mechanical properties of the formed parts, tensile tests were used. In addition precise cutting has to be done with the use of a wire cutting machine in order to guarantee accuracy of the tests. The wire cut machine creates fine and high quality samples. Figure 3.10 shows the wire cut machine during the process.

Figure 3.10: Wire-cut machine

Tensile samples were cut following ASTM standards. The figure 3.11 below illustrates the geometric specifications:

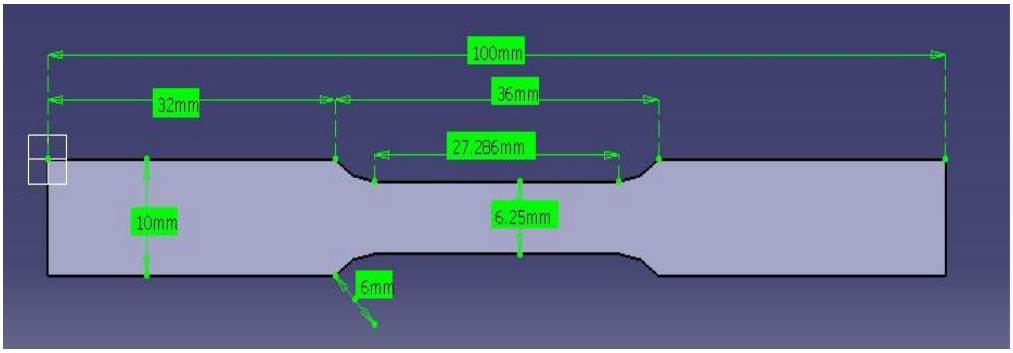

Figure 3.11: Dimensions of a tensile sample

In current experimental work, tensile tests were done by material testing machine made by Instron (as can be seen in figure 3.12) to investigate the mechanical properties of the formed sheets. The tension test provides primary but vital data to disclose the strength and the ductility of the material.

Figure 3.12: Instron tensile testing machine

Table 3.8: Properties of the materials

Material	AA5754-H22	AA6061-T6
Modulus of Elasticity (Young's modulus) (E)	70Gpa	68.9Gpa
Poison's ratio (υ)	0.33	0.33
Density (ρ)	2.66 g/cm³	2.7 g/cm³

Chapter 4

RESULTS AND DISCUSSION

In the current chapter the effects of the wall angle, feed rate, spindle speed and the lubrication are discussed to understand their effects on the microstructure and mechanical properties of parts manufactured by SPIF. The evaluations were done only for the samples along the forming direction of the SPIF by using a tensile test machine and optical microscopes. Totally, there were 17 tensile samples for tension test with the same amount for the optical microscopy to see compare the effects in both tests.

4.1 Effects of the Wall Angle

4.1.1 Effect of the Wall Angle on Mechanical Properties

The effects of wall angle on SPIF process was investigated by selecting 35º, 45º and 55º angles for the formed parts. The other parameters like feed rate, spindle speed and type of lubrication were held constant during this test. The figure 4.1 illustrates the difference of ultimate tensile strength values for both of the AA5754 and AA6061 Aluminium Alloys. As can be seen, by increasing the degree of wall angle, the values of the UTS will also be increased which initially has a greater increment from base material up to 35º wall angle later with higher wall angles again the amount of UTS increased but with lower slope.

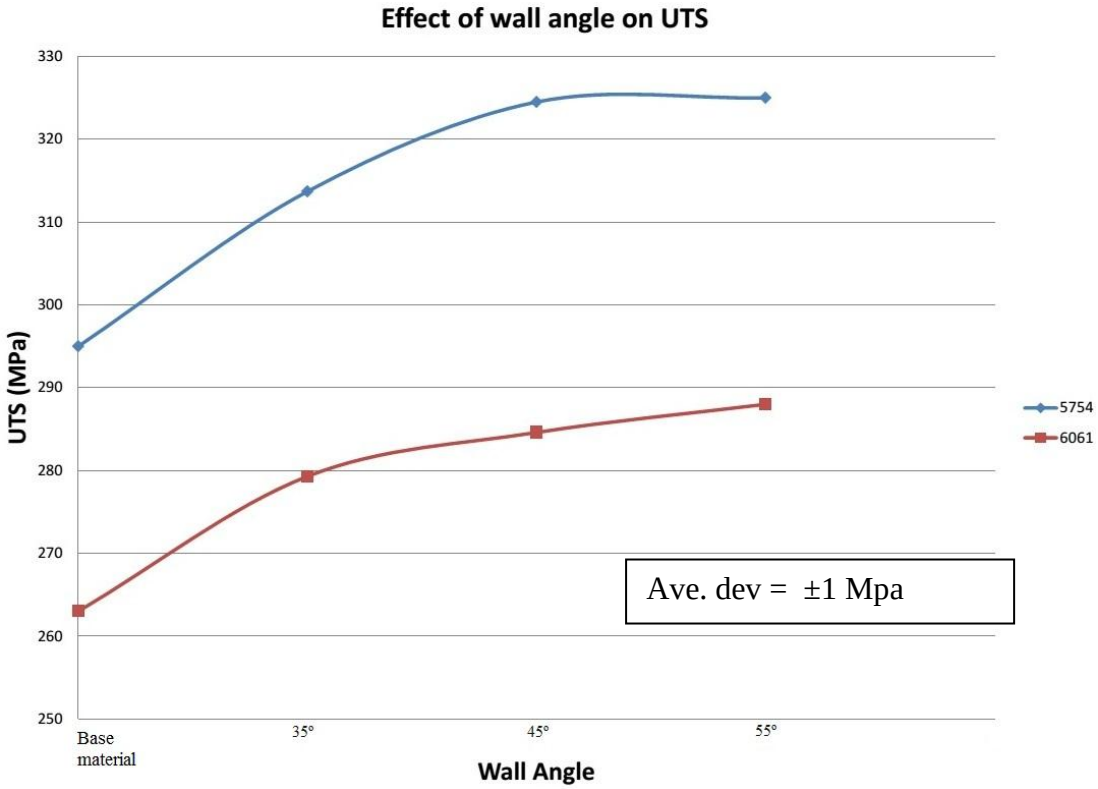

Figure 4.1: Effect of wall angle on the value of Ultimate tensile strength

This is because of the higher amount of cold work which leads to increase the work hardening and as a result the strength of the metal will be increased. But the values remain almost constant for the AA5754 from 45° till 55° wall angle. The figure 4.2 demonstrates the effects of 3 different wall angles on the ductility of the parts formed by SPIF. As can be seen, AA5754-H22 is more ductile than the AA6061-T6 material and there is a significant reduction in the amount of elongations in both materials, especially in AA5754 which dropped from 22.9% to 13.9%. By increasing the wall angle until 55º elongation also decreased to 12.8% and 10.7% for AA5754 and AA6061 respectively.

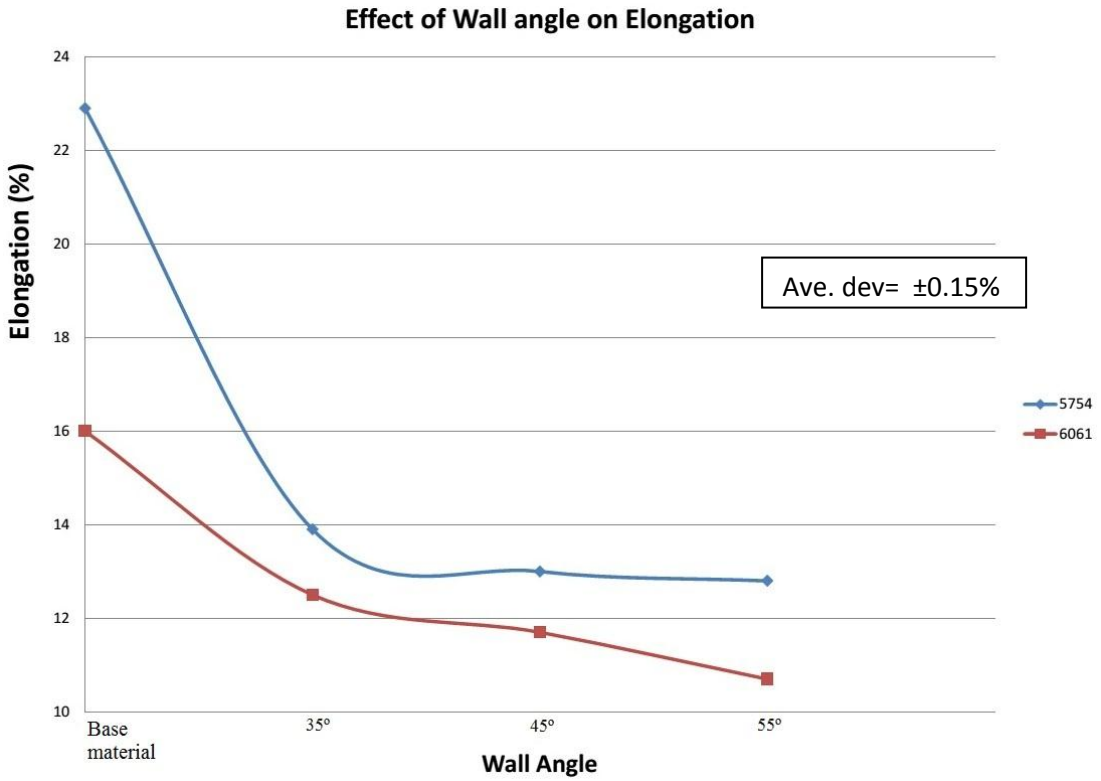

Figure 4.2: Effect of wall angle on the elongation

4.1.2 Effect of Wall Angle on Microstructure

This section presents the effect of different wall angle on microstructures of AA5754. In figure 4.3 shows the optical microscopic pictures of base material and the formed parts with 3 different wall angles. The average grain diameter for base material is 103 µm, figure 4.3 (A). After the forming process with 35º wall angle, figure 4.3 (B), the average grain diameters increased to 121 µm. According to the values of the average grain diameter and average grain area (Table 4.1), by increasing the wall angle the size of the grain also increases.

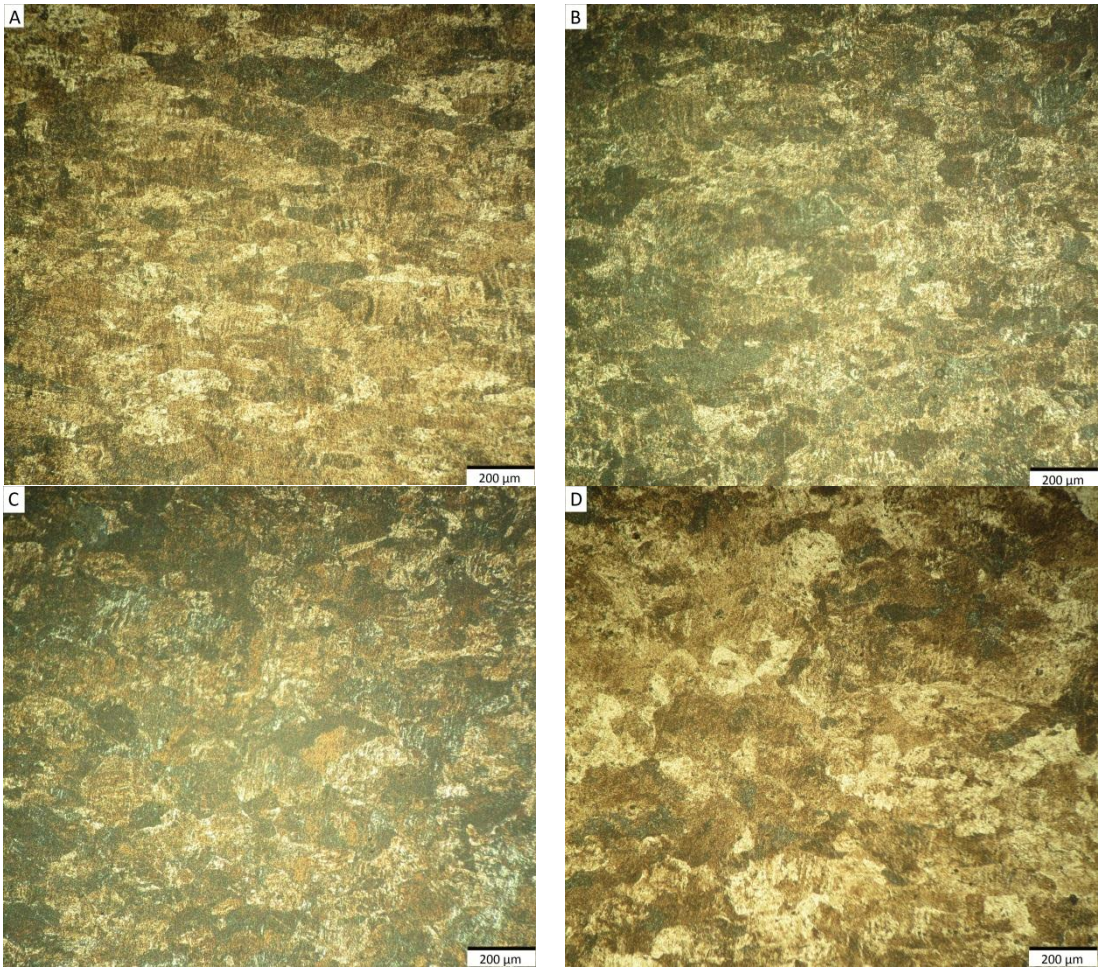

Figure 4.3: Effect of wall angle on AA5754 Aluminium Alloy with 100X magnification (A) base material, (B) 35º wall angle, (C) 45° wall angle, and (D) 55° wall angle

Table 4.1: Effect of wall angle on average grain size- Ave. deviation= ±1 µm

Wall angle of the formed part	Average grain diameter ($\bar{d}$) (µm)	ASTM grain size Number (G) [39]	Average grain area ($\bar{A}$) (µm^2)	Mean linear intercept length (l) (µm)
Base Material	103	3.6	10609	92.4
35º	121	3.1	14641	107.7
45°	142	2.6	20164	126.5
55°	149	2.5	22201	132.7

Different wall angles were investigated to discover the effect of them on second phase particles in AA6061. The chemical designation of the AA6061 sheet is AlMg1SiCu and according to the ASM Handbook Vol. 9 [38] these black particles are considered as Mg_2Si. As can be seen, figure 4.4(A) is the AA6061 before deformation and Mg_2Si particles are evenly distributed throughout the material. Figure 4.4 (B) Illustrates the least amount of joining of the second phase particles, on the other hand it possess the highest density of impurity.

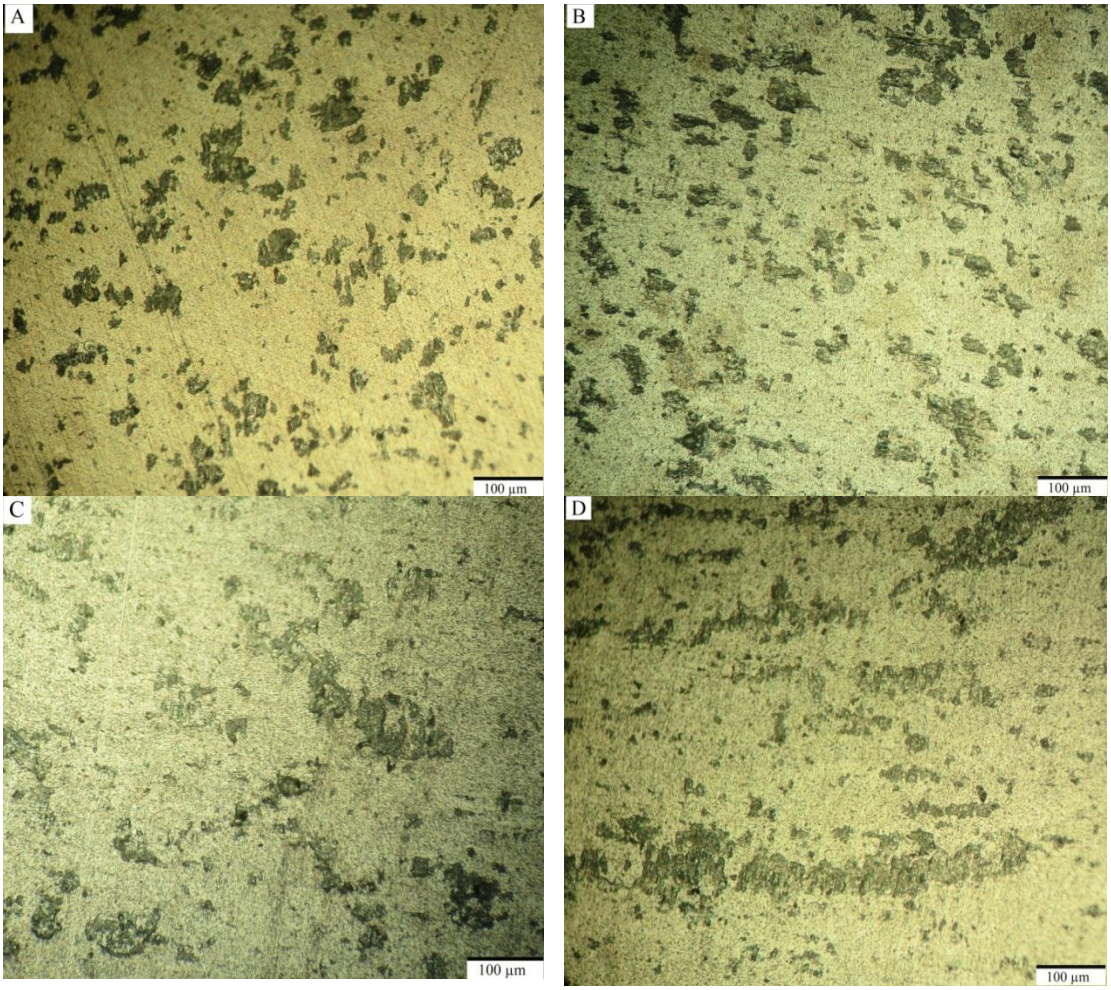

Figure 4.4: Effects of wall angle on AA6061 Aluminium Alloy with 200X magnification (A) base material, (B)35º wall angle, (C) 45° wall angle and (D) 55° wall angle

In figure 4.4 (D) the highest amount of joining of the second phase particles can be observed. The table 4.2 shows the maximum length and width of the second phase particles in each forming angle. It can be seen, the length of the Mg_2Si particles increased and stretched along the direction of forming tool during the SPIF process. So the distortion of these particles after forming lead to increase the maximum length of the particles from 783 µm to 4565 µm which is belong to the highest wall angle in this experiment.

Table 4.2: Effects of different wall angle on the length and width of the second phase particles in AA6061-Ave. deviation= ±6 µm

wall angle	Base material	35°	45°	55°
Length of the maximum Mg_2Si particles (µm)	783	1130	1864	4565
width of the maximum Mg_2Si particles (µm)	1000	435	818	652

4.2 Effects of the Feed rate

4.2.1 Effect of the Feed rate on Mechanical Properties

In this study in order to spot the effect of feed rate on SPIF process, 3 different feed rates have been used (1000, 2000 and 4000 mm/min). The rest of the parameters like wall angle, spindle speed and type of lubrication held constant. From the figure 4.5 it is clear that AA5754 has more strength than AA6061 in both before and after the plastic deformation. In case of AA5754, by increasing the amount of feed rate up to 4000mm/min strength of the material will also increase, and in AA6061 a constant increase is observed until the 4000 mm/min feed rate.

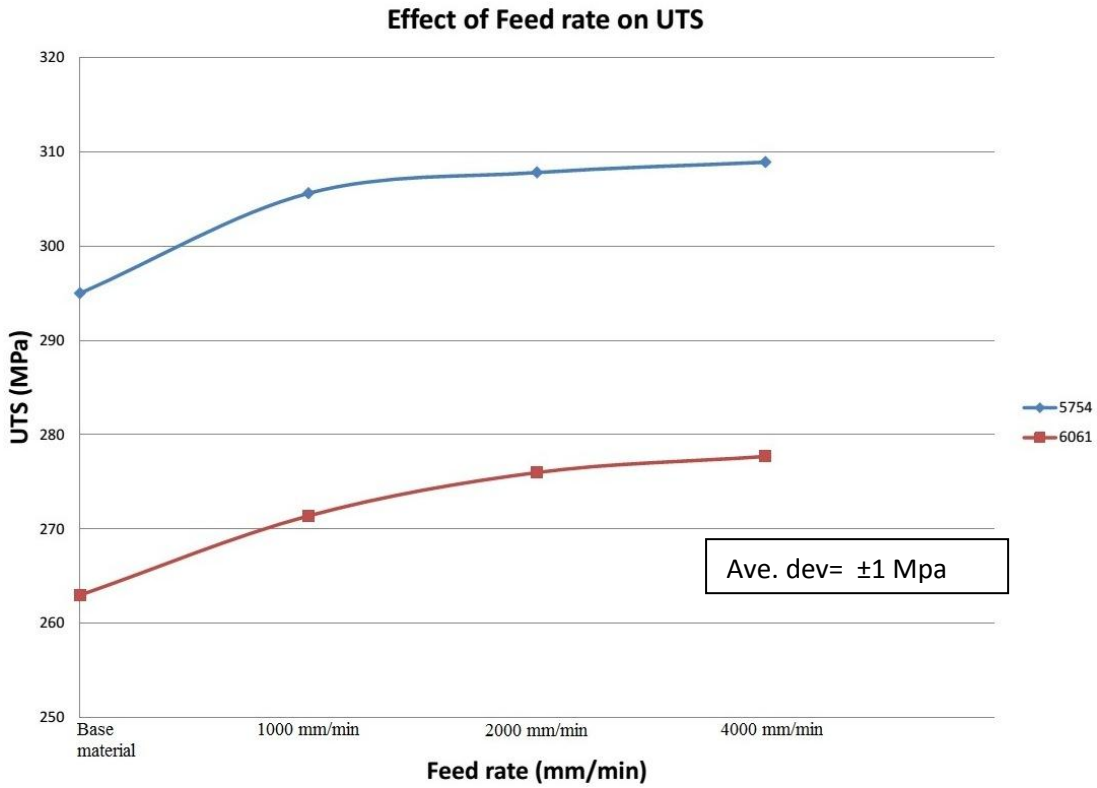

Figure 4.5: Effect of feed rate on the value of ultimate tensile strength

The figure 4.6 shows the effect of feed rate on elongation of the specimens. Due to work hardening, it is logical to expect a reduction in the amount of elongation after the plastic forming. The most reduction in ductility is observed in case of AA5754 which was from 22.9% to 13% belongs to the base material and formed material with 1000 mm/min. From 1000 to 4000 mm/min the values of elongation remain almost constant, which shows that feed rate has a little effect on the elongation of the parts formed by SPIF.

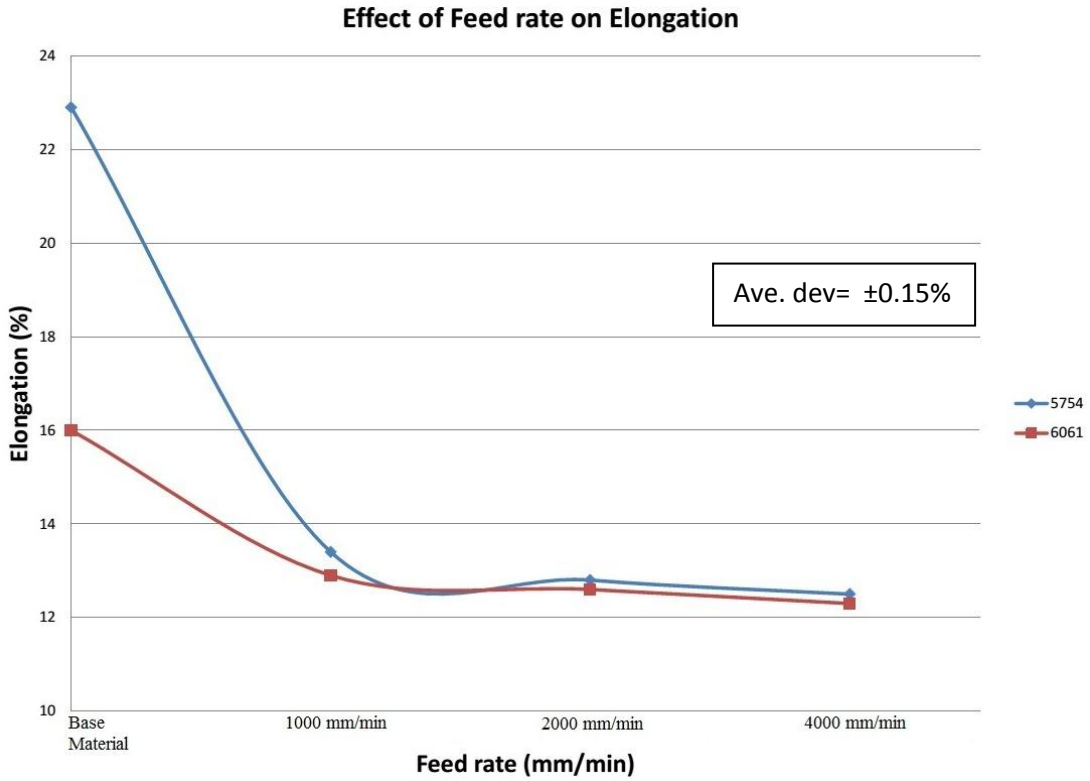

Figure 4.6: Effect of feed rate on the elongation

4.2.2 Effect of the Feed rate on Microstructures

The effect of feed rate on parts formed by SPIF process on microstructures is investigated in current section. Figure 4.7 illustrates the OM pictures of 3 different feed rates with the base material. As can be seen in figure 4.7 with higher feed rate, average grain diameter of the specimens increased from 116µm corresponding to 1000 mm/min feed rate, figure 4.7 (B), to 138µm which is formed with 4000 mm/min feed rate, figure 4.7 (D).

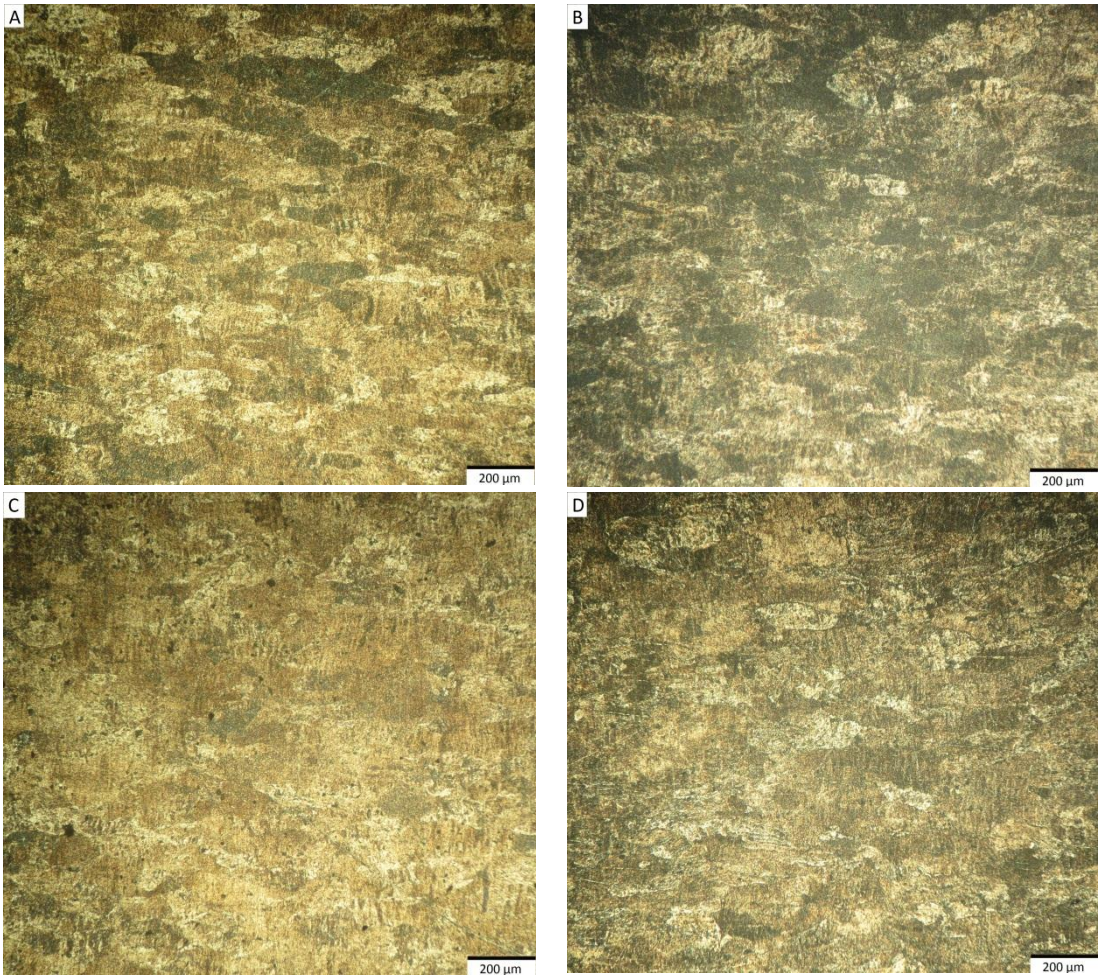

Figure 4.7: Effects of feed rate on AA5754 Aluminium Alloy with 100X magnification, (A) base material, (B) 1000 mm/min, (C) 2000 mm/min and (D) 4000 mm/min feed rate

Table 4.3: Effect of feed rate on average grain size- Ave. deviation= ±1 µm

Feed rate of the formed part	Average grain diameter ($\bar{d}$) (µm)	ASTM grain size Number (G) [39]	Average grain area ($\bar{A}$) (μm^2)	Mean lineal intercept length (l) (µm)
Base Material	103	3.6	10609	92.4
1000mm/min	116	3.2	13456	103
2000mm/min	125	3.0	15625	111.3
4000mm/min	129	2.9	16641	114

Also according to the ATSM standards for metallography [39], ASTM grain number of the each mounted specimen is determined and presented in the table 4.3. Also the average grain area and the mean lineal intercept length are provided for each sample.

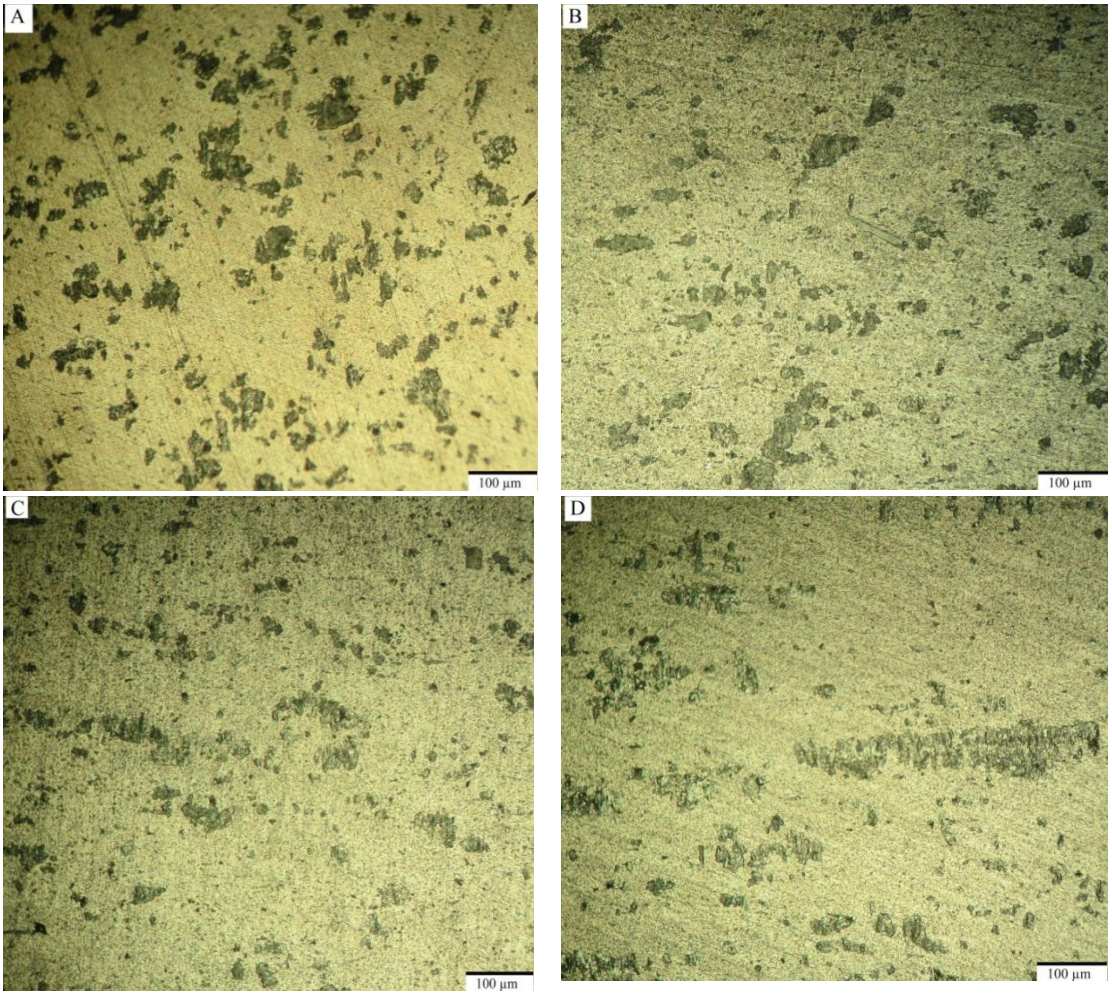

Figure 4.8: Effect of feed rate on AA6061 Aluminium Alloy with 200X magnification, (A) base material, (B) 1000 mm/min, (C) 2000mm/min, (D) 4000 mm/min feed rate

Based on the figure 4.8 it can be perceived that the amount of the impurities have been decreased after the forming process, but it seems that the density of second phase particles remains almost the same. The OM pictures illustrates that the feed rate has an effect on the joining of the second phase particles. With increasing the feed rate more elongated particles are observed. Table 4.4 displays the maximum

length and width of the Mg_2Si particles.

Table 4.4: Effect of feed rate on the length and width of the second phase particles in AA6061-Ave. deviation= ±6 µm

Feed rate	Base material	1000(mm/min)	2000(mm/min)	4000(mm/min)
Length of the max Mg_2Si particles (µm)	783	870	1000	4260
width of the max Mg_2Si particles (µm)	1000	826	435	869

4.3 Effects of the spindle speed

4.3.1 Effect of the Spindle speed on Mechanical Properties

This section investigates the effects of spindle speed on ultimate tensile strength by using 3 different rotational speeds during the forming process.

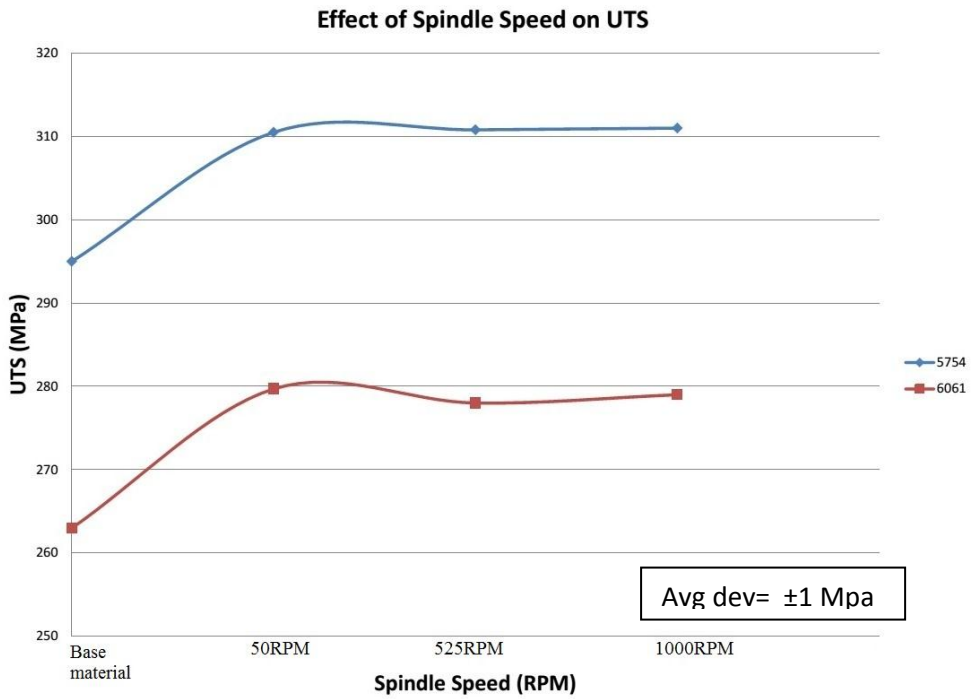

Figure 4.9: Effects of spindle speed on the value of ultimate tensile strength

The other parameters like wall angle, feed rate and lubrication type were held constant during this test. Figure 4.9 shows the increment in the strength of the material after the forming process in both materials. However, the UTS values from 50RPM to 1000RPM have slight changes in both AA5754 and AA6061, it can be realized that spindle speed has slight effect on the strength of the both materials formed by SPIF process.

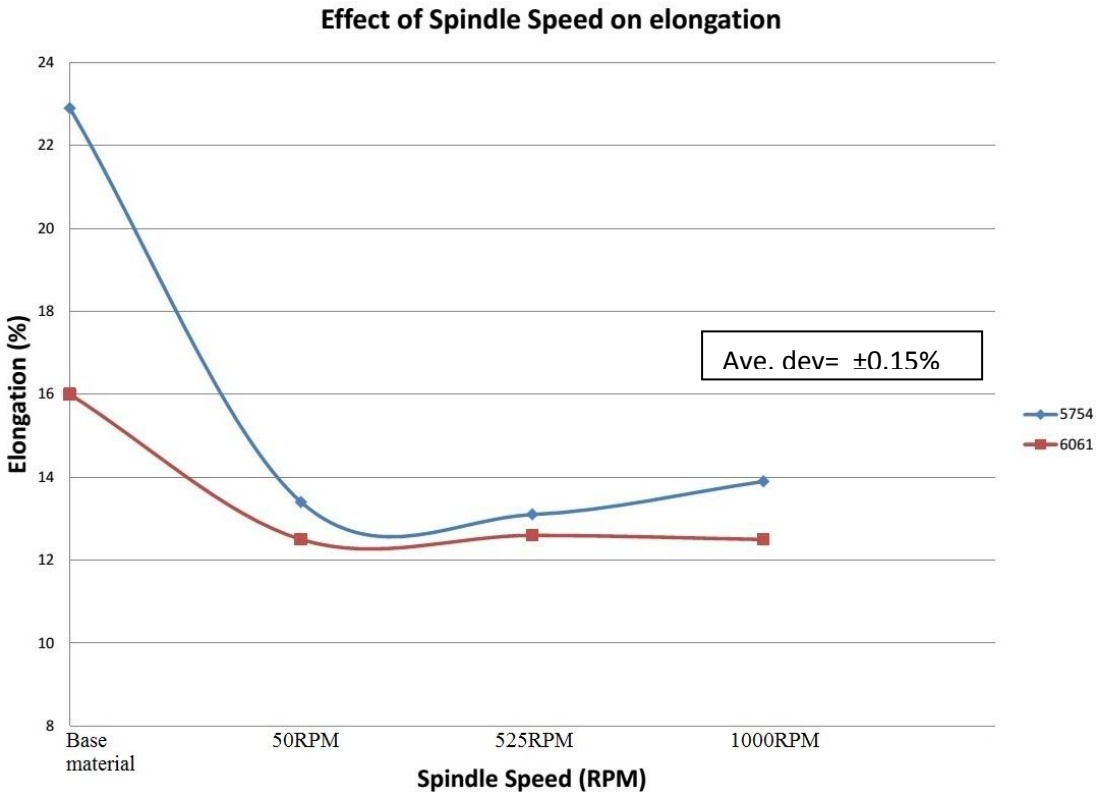

Figure 4.10 Effect of Spindle speed on the elongation

The figure 4.10 demonstrates the effects of spindle speed on the elongation of the formed parts. It can be realized that there is a significant reduction in the amount of the elongation after the forming process in both materials that is because of the work hardening that cause to reduce the ductility. From the graphs in figure 4.10 it can be seen that elongation in AA6061 remains almost constant until 1000RPM but there is a slight increment in case of AA5754 material in 1000RPM spindle speed.

4.3.2 Effect of the Spindle speed on Microstructure

This section examines the effect of spindle speed on microstructures of the AA5754. As can be seen in figure 4.11 the OM pictures of base material and 3 different spindle speeds are given. The average grain diameter for base material is 103µm, figure 4.11 (A). Based the values obtained from OM pictures, part which formed with 525RPM spindle speed has greater average grain diameter with compare to the others, figure 4.11 (C).

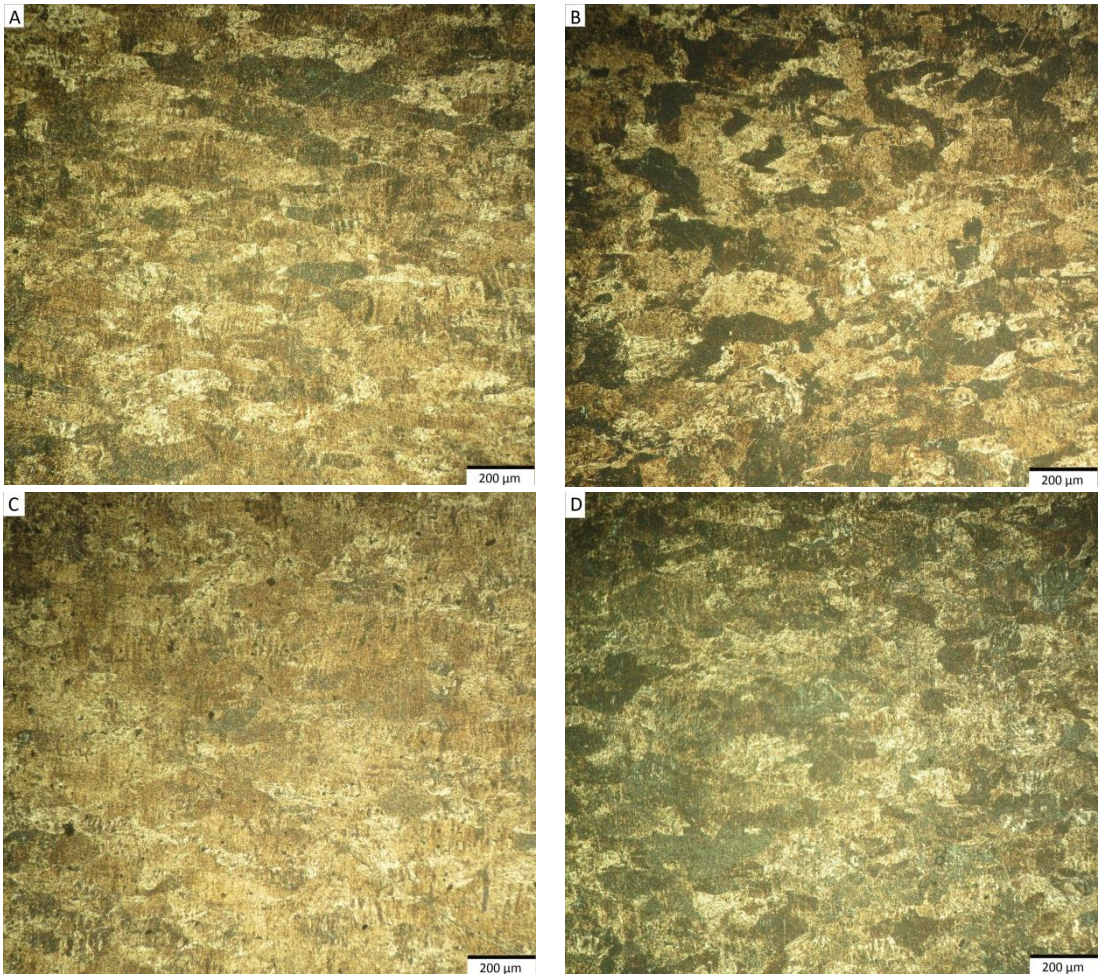

Figure 4.11: Effect of different spindle speeds on AA5754 Aluminium Alloy with 100X magnification, (A) base material, (B) 50 RPM, (C) 525 RPM and (D) 1000 RPM spindle speed

It can be said that average grain diameters and average grain area is increased until the 525RPM but these values reduced with the 1000RPM spindle speed, figure 4.11 (D).

Table 4.5: Effect of spindle speed on average grain size- Ave. deviation= ±1 µm

Spindle speed	Average grain diameter ($\bar{d}$) (µm)	ASTM grain size Number (G) [39]	Average grain area ($\bar{A}$) (μm^2)	Mean lineal intercept length ($\bar{l}$) (µm)
Base Material	103	3.4	10609	92.4
50RPM	108	3.4	11664	96.1
525RPM	125	3.0	15625	111.3
1000RPM	121	3.1	14641	107.7

Figure 4.12 displays the effects of the spindle speeds on the second phase particles in AA6061. Comparison between the base material and formed parts shows there is no significant effect on joining the Mg_2Si particles after the deformation. So the OM pictures reveal that the spindle speed in SPIF has the least effect on the elongation of the impurities in AA6061.

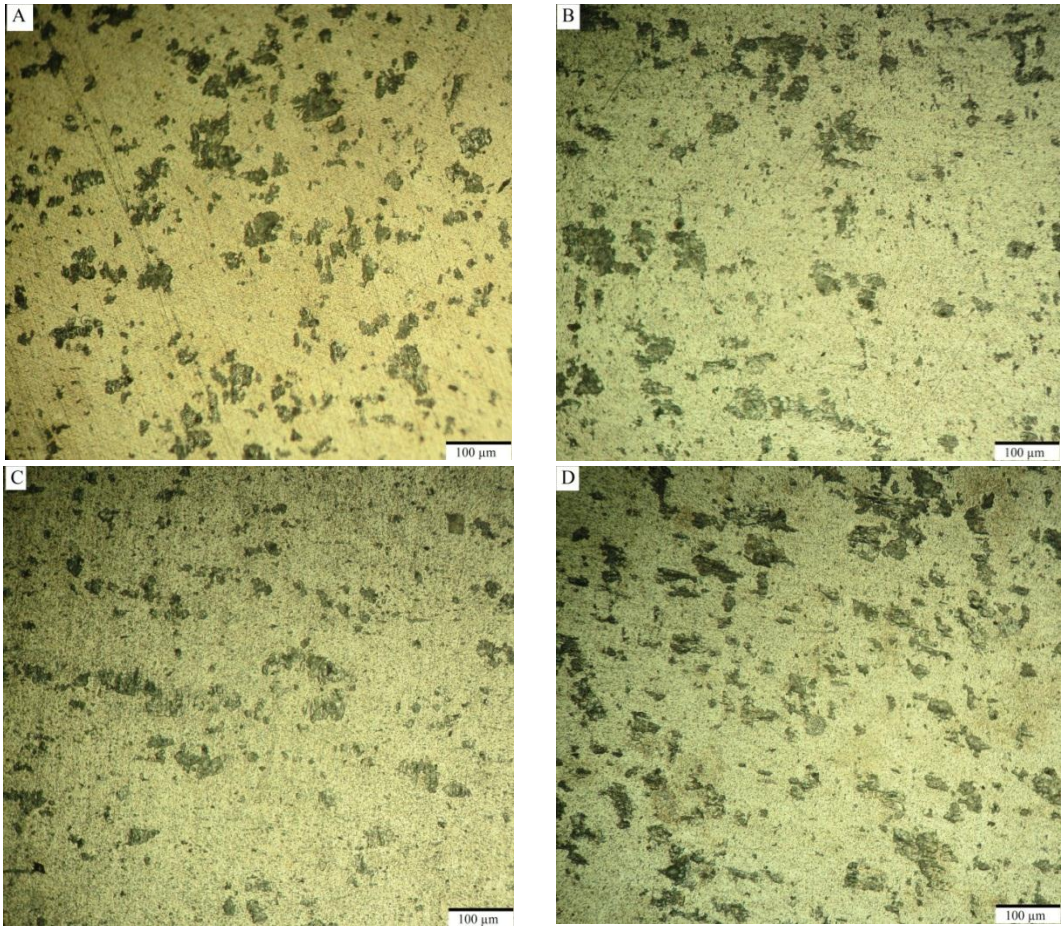

Figure 4.12: Effect of different spindle speeds on AA6061 Aluminium Alloy with 200X magnification, (A) base material, (B) 50RPM, (C) 525RPM and (D) 1000RPM spindle speed

Since the rotational speed of the spindle has direct effect on the generated heat during the process, the part formed with 1000 RPM (Figure 4.12 D) is expected to has higher temperature during the forming process; as a result this might explain the high density of the Mg_2Si particles along the formed part.

Table 4.6: Effects of different spindle speed on the length and width of the second phase particles in AA6061- Ave. deviation= ±6 µm

spindle speed	Base material	50 RPM	525 RPM	1000 RPM
Length of the maximum Mg_2Si particles (µm)	783	783	1000	1130
width of the maximum Mg_2Si particles (µm)	1000	826	435	435

4.4 Effects of the lubrication

4.4.1 Effect of the lubrication on Mechanical Properties

In this section effect of different lubrications is investigated. Hydraulic oil and lithium complex grease were selected to see their effects on the strength and the ductility of the formed parts. As can be seen in table 4.7 part formed with hydraulic oil has lower UTS than the one formed using grease. Also in case of ductility, specimen that formed with hydraulic oil has higher elongation with compare to the part formed with grease.

Table 4.7: Effects of lubricant on 5754 Aluminium Alloy

Lubrication	Base Material	Hydraulic oil	Grease
Ultimate tensile strength (UTS)-MPa	295	313.7	315
Elongation	22.9%	13.9%	13.1%

4.4.2 Effect of the lubrication on Microstructure

Figure 4.13 shows the OM pictures of 2 different lubrications, Hydraulic oil and Grease. It is observed that by replacing the grease instead of hydraulic oil with 121µm average grain diameter, figure 4.13 (B), the average grain diameter will tend

to increase up to 130µm, figure 4.13 (C). The table 4.8 provides the average grain area, ASTM number and means linear intercepts of both conditions with base material as a reference.

Figure 4.13: Effect of lubrications on AA5754 Aluminium Alloy with 100X magnification, (A) base material, (B) Hydraulic oil, (C) Grease.

Table 4.8: Effect of different lubricants on grain size- Ave deviation=±1 µm

Type of the lubrication	Average grain diameter ($\bar{d}$) (µm)	ASTM grain size Number (G)	Average grain area ($\bar{A}$) (µm^2)	Mean lineal intercept length (l) (µm)
Base Material	103	3.4	10609	92.4
Hydraulic oil	121	3.1	14641	107.7
Grease	130	2.9	16900	115.7

Chapter 5

CONCLUSION

The current research is done to investigate the effects of parameters in single point incremental forming process on the microstructures and mechanical properties of AA5754 and AA6061 Aluminium Alloys. The effects of variations in wall angle, feed rate, spindle speed and lubrication have been studied through practical tests. The following important results are obtained from this study:

1. Wall angle has a major effect on work hardening of the parts and as a result there is an increase in the strength of the both materials. The highest values for ultimate tensile strength are shown by the parts made with 55° wall angle. However, increase in wall angle leads to a reduction in the ductility. From microscopic observation, the average grain sizes and the length of the second phase particles increase with increasing the wall angle.
2. It is observed that a higher feed rate also increases the strength of the formed parts in both materials, because of the effects of the strain hardening during the process. Meanwhile, higher feed rates tend to increase the average grain size in the AA5754, likewise, the same effect is observed in the AA6061 which shows an increment in the maximum length of the Mg_2Si particles.
3. According to tensile tests and optical microscopy, the spindle speed has a slight effect on mechanical properties like strength and ductility. However,

there is a slight increment in the value of UTS in 1000RPM compared to the 50RPM which was the least spindle speed in this experiment.

4. The results for different lubricants show that using hydraulic oil instead of grease reduces the average grain size and increases elongation. However, parts produced with grease have a higher value of ultimate tensile strength.
5. Based on the findings, the wall angle and the feed rate are the most influential parameters affecting microstructure and mechanical properties of materials formed by SPIF process.
6. The reported findings will provide helpful guidance for material processing and product design.

REFERENCES

[1] Altan T., Tekkaya E. (2012). *Sheet Metal Forming : Fundamentals.* s.l. : ASM International.

[2] Altan T., Tekkaya E. (2012). *Sheet Metal Forming : Processes and Applications.* s.l. : A S M International.

[3] Kaufman, J.G. (2000). *Introducton to aluminum alloys and tempers.* s.l. : ASM International.

[4] Retrieved from: The Lincoln Electric Company. 2014 [Online]. http://www.lincolnelectric.com/.

[5] Retrieved from: The European Aluminium Association and MATTER. 2010 [Online]. http://aluminium.matter.org.uk/.

[6] Mohammed A. (2011). Automotive Body Manufacturing Systems and Processes. s.l. : John Wiley & Sons, 2011. 9780470978474.

[7] Retrieved from: CustomPartNet. 2014 [Online]. http://www.custompartnet.com/.

[8] Hagan E. and Jeswiet J. (2003). A review of conventional and modern single point sheet metal forming methods. *Journal of Engineering Manufacture*. 217- 213–225.

[9] Tisza M. (2012). General overview of sheet incremental forming. *Journal of Achievements in Materials and Manufacturing Engineering.* 55,113-120.

[10] Jadhav S. (2004). Basic Investigations of the Incremental Sheet Metal Forming Process on a CNC Milling Machine. Institut für Umformtechnik und Leichtbau, Germany.

[11] Rodrigues J.M.C., Martins P.A.F. (2005). Tecnologia daDeformação Plástica: Aplicações Industriais, Escolar Editora.

[12] Silva MB, Skjoedt M, Atkins AG, Bay N, Martins P.A.F. (2008). Single Point Incremental Forming & Formability/Failure Diagrams. *Journal of Strain Analysis for Engineering Design* 43(1):15–36.

[13] Silva M.B. (2008). Single Point Incremental Forming. PhD Thesis, Instituto Superior Técnico Portugal.

[14] Martins P.A.F., Bay N., Skjoedt M., Silva M.B. (2008). Theory of single point incremental forming. CIRP Annals – *Manufacturing Technology*. 57-247-252.

[15] Nakajima K., Kikuma T. (1967). Forming limits under balanced biaxial stretching of steel sheets. *Tetsu-to-Hagane.* 53/4- 455-458.

[16] Marciniak Z. (1965). Stability of plastic shells under tension with kinematic boundary conditions, *Archives of Mechanical.* 17,577-592.

[17] Hussain G., Gao L., Hayat N. (2011). Forming Parameters and Forming Defects in Incremental Forming of an Aluminum Sheet: Correlation, Empirical Modeling, and Optimization: Part A. *Materials and Manufacturing Processes*. 12, 1546-1553.

[18] Park J., Kim Y.-H. (2003). Fundamental studies on the incremental sheet metal forming technique. *Journal of Materials Processing Technology*. 140, 447–453.

[19] Ham M, Jeswiet J. (2006). Single point incremental forming and the forming criteria for AA3003, *CIRP Annals*. 55, 241-244.

[20] Bhattacharya A., Maneesh K., Venkata N., Cao J. (2011). Formability and Surface Finish Studies in Single Point Incremental Forming. *Journal of Manufacturing Science and Engineering.*133- 061020.

[21] Y.H. Kim, J.J. Park . (2011). Effect of process parameters on formability in incremental forming of sheet metal. *Journal of Manufacturing Science and Engineering, Transactions of the ASME*. ;133, 341-344.

[22] Iseki H., Kumon H. (1994). Forming limit of incremental sheet metal stretch forming using spherical rollers, *Journal of JSTP*. 35, 1336.

[23] Hussain G., Gao L. (2007). A novel method to test the thinning limits of sheet metals in negative incremental forming. *International Journal of Machine Tool and Manufacturing.* 47, 419–435.

[24] Strano M. (2005). Technological Representation of Forming Limits for Negative Incremental Forming of Thin Aluminum Sheets. Journal of Manufacturing Processes. 7, 122-129.

[25] Hussain G., Dar N.U., Gao L., Chen M.H. (2007). A comparative study on the forming limits of an aluminum sheet-metal in negative incremental forming. *Journal of Materials Processing Technology*. 187–188, 94–98.

[26] Strano, M., Sorrentino, L., Carrino, L. (2004). Some issues about tools and friction in the negative dieless incremental forming process. Steel Grips 2 Metal Forming Supplement. 345–349.

[27] Nimbalkar D.H and Nandedkar V.M. (2013). Review of Incremental Forming of Sheet Metal Components Review of Incremental Forming of Sheet Metal Components. *Journal of Engineering Research and Applications.*3, 39-51.

[28] Jeswiet J., Micari F., Hirt G., Bramley A, Duflou J, Allwood J. (2005). Asymmetric Single Point Incremental Forming of Sheet Metal-CIRP Annals manufacturing technology, ,54(2),623-649.

[29] Hagan, E., Jeswiet, J. (2004). Analysis of surface roughness for parts formed by computer numerical controlled incremental forming. Proc. IMechE. J. Engineering Manufacture. 218, 1307-1312.

[30] Silva M.B., Skjoedt M., Martins P.A.F., Bay N. (2008). Revisiting the fundamentals of single point incremental forming by means of membrane analysis. *International Journal of Machine Tools & Manufacture*. 48, 73-83.

[31] Skjøedt M. (2008). Rapid Prototyping by Single Point Incremental Forming of Sheet Metal, PhD Thesis, Technical University of Denmark.

[32] Amino, H, Lu, Y, Ozawa, S, Fukuda, K, Maki, T. (2002). Dieless forming of automotive service panels. Proc. 7th ICTP, Oct 28-31, Yokohama, Japan, pp. 1015-1020.

[33] Jeswiet J. (2004). Recent results for SPIF. Seminar on Incremental Forming, Cambridge University CdRom.

[34] Rauch M. (2009). Tool path programming optimization for incremental sheet forming applications. *Journal of Computer-Aided Design.* 41, 877-885.

[35] Suresh K., Khan A., Regalla S.P. (2013). Tool path definition for numerical simulation of single point incremental forming. *International Conference on Design and Manufacturing.* 64, 536 -545.

[36] Allwood J.M., Shouler D.R., Tekkaya A.E. (2007). The increased forming limits of incremental sheet forming processes. Key Engineering Materials. 344, 621-628.

[37] Fuller C.B., Krause A.R., Dunand D.C., Seidman D.N., (2002). Microstructure and mechanical properties of a 5754 aluminum alloy modified by Sc and Zr additions. *Materials Science and Engineering.* A338, 8-16.

[38] Mills K., Davis J.R., Destefani J.D. (1985). Metallography and Microstructures. ASM Handbook, vol. 9.

[39] American Society for Testing of Materials, ASTM. (2000). Standard test methods for determining the average grain size. ASTM E 112 – 96.

APPENDICES

Appendix A: G Codes for the Helical Tool Path with 35° Wall Angle

%

G17 G21 G40 G49 G80 G54 G90

G5. 1 Q1

S1000M3

G00X0 Y0 Z50 M8

G01X80 Y80 Z0 F2000

X -79.8215 Y 79.8215 Z -0.125

X -79.643 Y -79.643 Z -0.25

X 79.4645 Y -79.4645 Z -0.375

X 79.286 Y 79.286 Z -0.5

X -79.1075 Y 79.1075 Z -0.625

X -78.929 Y -78.929 Z -0.75

X 78.7505 Y -78.7505 Z -0.875

X 78.572 Y 78.572 Z -1

X -78.3935 Y 78.3935 Z -1.125

X -78.215 Y -78.215 Z -1.25

X 78.0365 Y -78.0365 Z -1.375

X 77.858 Y 77.858 Z -1.5

X -77.6795 Y 77.6795 Z -1.625

X -77.501 Y -77.501 Z -1.75

X 77.3225 Y -77.3225 Z -1.875

X 77.144 Y 77.144 Z -2

X -76.9655 Y 76.9655 Z -2.125

X -76.787 Y -76.787 Z -2.25

X 76.6085 Y -76.6085 Z -2.375

X 76.43 Y 76.43 Z -2.5

X -76.2515 Y 76.2515 Z -2.625

X -76.073 Y -76.073 Z -2.75

X 75.8945 Y -75.8945 Z -2.875

X 75.716 Y 75.716 Z -3

……

X 30.9125 Y -30.9125 Z -34.375

X 30.734 Y 30.734 Z -34.5

X -30.5555 Y 30.5555 Z -34.625

X -30.377 Y -30.377 Z -34.75

X 30.1985 Y -30.1985 Z -34.875

X 30.02 Y 30.02 Z -35

G00Z100

X0 Y240

M2

M9

%

Appendix B: Drawing of the Clamping System (Upper plate)

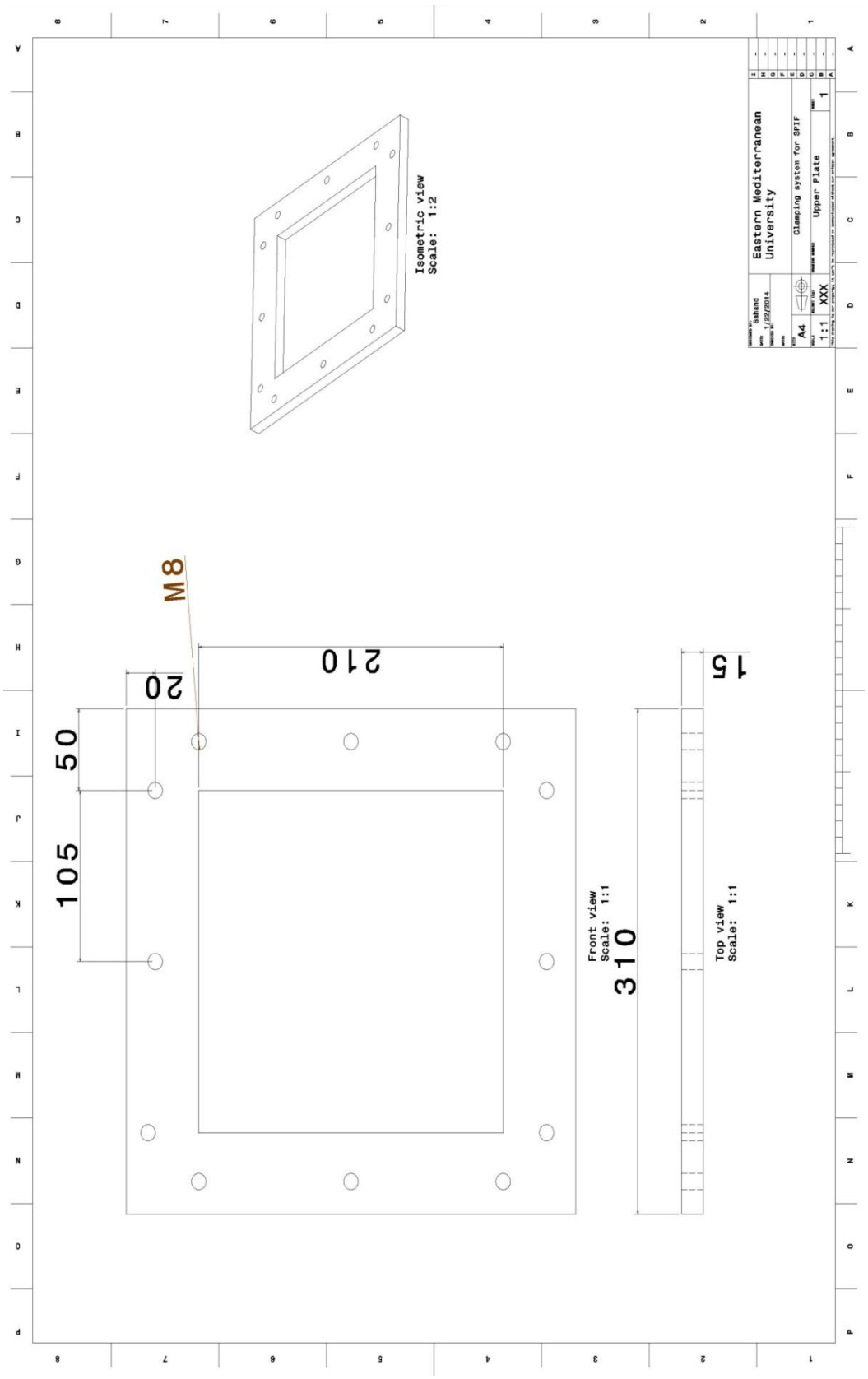

Appendix C: Drawing of the Clamping System (Lower plate)